UDK/UDC: 621.791 **ISSN 0354-7965**

ZAVARIVANJE I ZAVARENE KONSTRUKCIJE

WELDING & WELDED STRUCTURES

God. 66	Br. 3	97-144	Beograd	Srbija	2021.
Vol. 66	No. 3	97-144	Belgrade	Serbia	2021.

ČASOPIS DRUŠTVA ZA UNAPREĐIVANJE ZAVARIVANJA U SRBIJI

SERBIAN WELDING SOCIETY QUARTERLY REVIEW

IZLAZI TROMESEČNO

IZDAVAČ / PUBLISHER

DUZS - Društvo za unapređivanje zavarivanja u Srbiji

Adresa: 11000 Beograd, Grčića Milenka 67

Za izdavača / For Publisher

Branislav Lukić, dipl.ing, predsednik DUZS

UREĐIVAČKI ODBOR / PUBLISHING COUNCIL

Dr Vencislav Grabulov, dipl.ing, (predsednik)

Prof.dr Vukić Lazić, dipl.ing.

Doc.dr Ismar Hajro, dipl.ing. (BiH)

Prof.dr Darko Bajić, dipl.ing. (Crna Gora)

Prof. dr Dragoslav Dobraš, dipl.ing. (BiH, Republika Srpska)

Prof. dr Sveto Cvetkovski, dipl.ing. (Makedonija)

Doc. dr Tomaž Vuherer, dipl.ing. (Slovenija)

Prof. dr Ivan Samardžić, dipl.ing. (Hrvatska)

Dr Horia Dascau, dipl.ing. (Rumunija)

UREDNIŠTVO / EDITORIAL

Glavni i odgovorni urednik / Editor-in-Chief

Dr Zoran Odanović, dipl.ing.

duzs011@gmail.com, odanovic@ptt.rs

Tehnički urednik / Technical Editor

Branislav Lukić, dipl.ing

Redakcijski odbor / Editorial Board

Dr Nenad Radović, dipl.ing.

Dr Radomir Jovičić, dipl.ing.

Dr Bore Jegdić, dipl.ing.

Miloš Pavlović, dipl.ing.

REDAKCIJA I MARKETING / EDITORIAL OFFICE AND MARKETING

Vesna Jović
Grčića Milenka 67, I sprat
11000 Beograd

Tel / Fax + 381 (11) 2420-652
(10-16h)

duzs@eunet.rs
www.duzs.org.rs

CIP - Каталогизација у публикацији
Народна библиотека Србије, Београд

621.791

ZAVARIVANJE i zavarene konstrukcije : časopis Društva za unapređivanje zavarivanja u Srbiji = Welding & Welded Structures : Serbian Welding Society quarterly review / glavni i odgovorni urednik Zoran Odanović. – Vol. 41, no. 1 (1996)- . - Beograd : DUZS - Društvo za unapređivanje zavarivanja u Srbiji, 1996-. (Beograd : VIS studio).-29 cm

Tromesečno. Je nastavak: Zavarivač = 0513-8523
ISSN 0354-7965 = Zavarivanje i zavarene konstrukcije
COBISS.SR-ID 105396743

CENE I NARUDŽBINA ZA 2021.

Cena pojedinačnog broja 825,00 dinara
Godišnja pretplata 2500,00 dinara
Tekući račun: 325-9500600002588-46

PRICE AND ORDER

Annual subscription: EUR 100
Account No. RS35325960160000041546
OTPVRS22 (VOJVOĐANSKA BANKA AD)
IBAN RS35325960160000041546

ŠTAMPA / PRINTED

"VIS STUDIO" d.o.o.
Bulevar Arsenija Čarnojevića 123, Beograd
Tiraž: 400 kom.

Časopis sufinansira Ministarstvo prosvete, nauke i tehnološkog razvoja Republike Srbije

Na osnovu mišljenja Ministarstva za nauku, tehnologije i razvoj Republike Srbije br. 413-00-2272/2001-01, časopis ZAVARIVANJE I ZAVARENE KONSTRUKCIJE je publikacija od posebnog interesa za nauku

3/2021

SADRŽAJ CONTENTS

NAUKA•ISTRAŽIVANJE•RAZVOJ SCIENCE•RESEARCH•DEVELOPMENT

101 **UTICAJ BORA I MANGANA NA OTPORNOST KA TOPLIM PRSLINAMA I ŽILAVOST ELEKTROLUČNO ZAVARENIH SPOJEVA PUNJENOM ELEKTRODNOM ŽICOM ČELIKA KLASE ZATEZNE ČVRSTOĆE OD 550 MPa** / **EFFECT OF BORON AND MANGANESE ON HOT CRACK RESISTANCE AND TOUGHNESS FOR FLUX CORED ARC WELDMENTS OF 550 MPa GRADE TENSILE STRENGTH**

S.K. Park, Y.H. Cho, C.H. Jee, N. Kang

PRAKSA PRACTICE

123 **HIBRIDNO LASERSKO ELEKTROLUČNO ZAVARIVANJE – PREGLED STANJA TEHNOLOGIJE** / **HYBRID LASER ARC WELDING – STATE OF THE ART IN TECHNOLOGY**

M. Petreski, D. Runchev, G. Vrtanoski

PRAKSA PRACTICE

125 **UTICAJ OBRADE OTPUŠTANJEM NAKON ZAVARIVANJA NA OSOBINE TAČKASTO ZAVARENOG SPOJA DVOFAZNOG ČELIKA DP DP600** / **EFFECT OF POST-WELD TEMPERING TREATMENT ON PERFORMANCE OF DP600 SPOT WELDED JOINT**

L. Hong, L. Xusheng, W. Bing, L. Zhuoxin

IBR (PRAKSA) NDT (PRACTICE)

133 **KONTROLISANJE ZAOSTALIH NAPONA: RAZVOJ NAJNOVIJIH INŽENJERSKIH METODA ZA MERENJE BEZ RAZARANJA I POVOLJNU PRERASPODELU ZAOSTALIH NAPONA** / **RESIDUAL STRESS MANAGEMENT: RECENT ADVANCES IN ENGINEERING METHODS FOR NON-DESTRUCTIVE MEASUREMENT AND BENEFICIAL REDISTRIBUTION OF RESIDUAL STRESSES**

J. Kleiman

VESTI NEWS

99 **68. GODIŠNJA SKUPŠTINA DUZS**
114 **68. GODIŠNJA SKUPŠTINA DUZS**
144 **MARKETING**

68. GODIŠNJA SKUPŠTINA DRUŠTVA ZA UNAPREĐIVANJE ZAVARIVANJA U SRBIJI
Beograd, 29.06.2021.

Ovogodišnja redovna, 68. godišnja skupština Društva za unapređivanje zavarivanja u Srbiji (DUZS), održana je 29. juna 2021. godine u svečanoj sali Instituta IMS u Beogradu.

Rad skupštine je počeo minutom ćutanja u znak poštovanja i sećanja na sve kolege preminule u prethodnom periodu.

Skupštinom je predsedavao Branislav Lukić, predsednik DUZS, a prisustvovalo je 33 člana. Podneti su izveštaji o radu DUZS, DUZS-CertPers i finansijskom poslovanju u 2020. godini, odakle izdvajamo sledeće podatke:

Tokom 2020. godine, na vreme su izašla sva četiri broja časopisa Zavarivanje i zavarene konstrukcije u ukupnom obimu od 192 strane. U izveštajnom periodu, za glavnog i odgovornog urednika časopisa izabran je Dr Zoran Odanović, dipl.ing. Status časopisa za 2020. godinu je M52 – Časopis nacionalnog značaja.

U prethodnoj godini, usled situacije izazvane pandemijom, nisu održane planirane aktivnosti DUZS - organizacija seminara, savetovanja i takmičenja mladih zavarivača. Termin savetovanja pomeren je na oktobar ove godine i ukoliko okolnosti dozvole, biće održano u Kladovu, kako je prvobitno i planirano.

Što se tiče međunarodne saradnje u proteklom periodu, DUZS je sarađivao sa Društvom za tehniku zavarivanja iz Slavonskog Broda, kao i sa Rumunskim društvom za zavarivanje, o čijim aktivnostima je bilo reči i u časopisu Zavarivanje i zavarene konstrukcije br. 2/2021.

U izveštajnom periodu, u svih 5 ovlašćenih centara za obuku (ATB), završeno je ukupno 5 kurseva za međunarodne / evropske inženjere i tehnologe zavarivanja i 3 kursa za međunarodne inspektore zavarivanja.

DUZS-CertPers-u je dodeljen sertifikat da može da obavlja aktivnosti Sertifikacionog tela za sertifikaciju zavarivačkog osoblja, čime je dobio mogućnost izdavanja sertifikata pod okriljem IIW-a.

Od 01. januara 2020. godine Generalni sekretarijat IIW-a se iz Pariza preselio u Đenovu. Novi tim upravlja Generalnim sekretarijatom IIW-a, a Luca Costa je novi Izvršni direktor.

Godišnja skupština IIW-a trebalo je da se održi u Singapuru, ali zbog pandemije COVID-19, održana je online od 15. do 26. jula 2020. godine. Ovom prilikom je prvi put u istoriji dugoj 73 godine predstavnik Srbije, dr Vencislav Grabulov, izabran da bude član Borda direktora IIW.

Nadzorni odbor je na osnovu razmatranja finansijskog i materijalnog poslovanja Društva, odnosno uvida u finansijski izveštaj DUZS po godišnjem računu za 2020. godinu, konstatovao da nije uočio nepravilnosti u radu. Informacije u vezi bilansa stanja i bilansa uspeha mogu se pronaći na internet stranici APR-a

Svi podneti izveštaji su usvojeni.

Usvojeni su i planovi rada DUZS i DUZS-CertPers za naredni period:

PLAN RADA DUZS:

IZDAVAČKA DELATNOST
• Časopis Zavarivanje i zavarene konstrukcije
• WEB prezentacija DUZS
SARADNJA SA SRODNIM ORGANIZACIJAMA:
• SDIBR, SMEITS, DIVK
SAVETOVANJE SA MEĐUNARODNI UČEŠĆEM „ZAVARIVANJE 2020“:
• Kladovo, Oktobar 2021
ORGANIZACIJA STRUČNIH SEMINARA:
• Stručni seminar, proleće 2022.
TAKMIČENJE MLADIH ZAVARIVAČA:
• Organizacija, proleće (maj) 2022.
REGIONALNA (MEĐUNARODNA) SARADNJA
• Učešću u radu EWF
• Učešće u radu regionalne grupe IIW za saradnju
• Učešće na međunarodnom takmičenju mladih zavarivača
• Saradnja sa Društvom za tehniku zavarivanja, Slavonski Brod
• Saradnja sa rumunskim društvom za zavarivanje - Romanian Welding Society

PLAN RADA DUZS-CertPers:

• Nastaviti praćenje relevantnih dokumenata i uz saradnju sa ATB održati visok nivo kurseva

• Isticati potrebu obrazovanja kadrova po pravilima IIW

• Dodatno angažovanje na organizaciji kurseva za IWS i IWP

• Učešće u radu komisija IAB grupa, posebno na harmonizaciji ispitnih pitanja i ispita i u delu izmene statusnih promena IAB grupe.

• Učešće na godišnjim sastancima IAB grupe

• Učešće u radu tehničkog komiteta EWF odnosno sastancima članova IAB grupe MIZ-a iz Evrope

• Implementacija pravila izdavanje sertifikata međunarodnim/evropskim inženjerima, tehnolozima ili inspektorima

• Ocena i usaglašavanje materijala za učenje svih ATB-ova

Nastavak na strani 114

Su-Kil Park [1,a], Young-Ho Cho [1,b], Chun-Ho Jee [1,c], Namhyun Kang [2,d]

Effect of boron and manganese on hot crack resistance and toughness for flux cored arc weldments of 550 MPa grade tensile strength

Uticaj bora i mangana na otpornost ka toplim prslinama i žilavost elektrolučno zavarenih spojeva punjenom elektrodnom žicom čelika klase zatezne čvrstoće od 550 MPa

Originalni naučni rad / Original scientific paper

Rad je u izvornom obliku objavljen u okviru 72. IIW godišnje Skupštine i međunarodne konferencije održane u Bratislavi-Slovačka 07-12. Jula 2019

Rad primljen / Paper received:
Decembar 2020.

Prevod izvornog rada na srpski jezik: A. Mitrašinović

Adresa autora / Author's address:

[1] Welding Research Dep't, Hyundai Heavy Industries Co., Ltd., Ulsan, Republic of Korea

[2] Department of Materials Science & Engineering, Pusan National University, Busan, Republic of Korea

[a] psk2011@hhi.co.kr,

[b] choyh@hhi.co.kr,

[c] jee1005@hhi.co.kr,

[d] nhkang@pusan.ac.kr

Keywords: hot crack resistance, low temperature toughness, self-restraint testing, boron, manganese

Ključne reči: otpornost na tople prsline, žilavost pri niskim temperaturama, ispitivanje zavarljivosti, bor, mangan

Abstract

The hot crack resistance and mechanical properties of flux cored arc (FCA) welds were investigated with three kinds of welding consumables having different boron (B) and manganese (Mn) contents for high strength carbon steel. The hot crack resistance measured from self-restraint testing strongly depended on the amount of B in the welding consumable. Welding consumable with higher B contents resulted in longer total crack length and an increased number of cracks. Boron was intensely detected near the grain boundary of the weld centerline by secondary ion mass spectrometry (SIMS) analysis, and precipitated with boron carbide ($Fe_{23}(C,B)_6$), as analyzed by transmission electron microscopy (TEM). This promoted hot crack propagation in the high strength carbon steel welds.

However, removing B from the welding consumable decreased the low temperature toughness for root and face weld metal due to the growth of Ferrite Side Plate (FSP) in comparison with welding consumables having more B or Mn contents. The addition of Mn in the weld metal suppressed the formation of FSP and increased the low temperature toughness. Therefore, the minimization of B and the supplement of Mn

Rezime

Otpornost ka stvaranju toplih prslina i mehaničke osobine elektrolučno zavarenih spojeva sa punjenim elektrodnim žicama (FCA) je ispitivano sa tri vrste žica sa različitim količinama bora (B) i mangana (Mn) za zavarivanje ugljeničnog čelika visoke čvrstoće. Otpornost ka toplim prslinama je merena primenom testova zavarljivosti, i jako je zavisila od količine B u upotrebljenom dodatnom materijalu za zavarivanje. Punjene elektrodne žice za zavarivanje sa većim sadržajem B rezultirale su varovima sa povećanim brojem i većom dužinom prslina. Bor je intenzivno detetkovan uz granice zrna duž središnje linije vara i određivan je metodom sekundarne jonske masene spektrometrije (SIMS). On se taložio u obliku bor-karbida ($Fe_{23}(C, B)_6$), što je utvrđeno transmisionom elektronskom mikroskopijom (TEM).

To je podstaklo dalje širenje toplih prslina u varovima ugljeničnog čelika visoke čvrstoće. Međutim, uklanjanjem bora iz dodatnog materijala smanjivala se žilavost na niskim temperaturama korenog i pokrivnog metala vara, zbog rasta feritnih lamela. Međutim, u poređenju sa upotrebljenim punjenim elektrodnim žicama koje sadrže B ili Mn, uklanjanjem B iz punjenih elektrodnih žica, smanjila se žilavost na niskim temperaturama osnovnog i površinskog metala vara zbog rasta bočnih feritnih

successfully achieved hot crack resistance and low temperature toughness for high strength carbon steel welds of 550 MPa tensile strength.

1. Introduction

Hot cracking occurs when sensitive microstructure for cracking and tensile stress due to shrinkage and external restraint of the weld at high temperature exceeding 300 ℃ during or immediately after welding is encountered.

The main cause of hot cracking is known as the austenite matrix of the face-centered cubic (FCC) crystal structure having a low solubility of phosphorus (P) and sulfur (S), and austenitic stainless steels and high alloy steels such as nickel alloys have been focused on hot cracking [1].

The purpose of this study is to evaluate the effect of boron (B) contents for hot cracking on Flux Cored Arc (FCA) weld metal for high strength carbon steel. Especially, the change of mechanical properties according to the content of boron was examined to prevent hot cracking and to secure mechanical properties by adjustment of chemical composition such as manganese (Mn).

2. Materials and experimental procedures

2.1 Base metal and welding condition

The base metal used in this study is high strength carbon steel (Grade: AH36) manufactured by Thermo-Mechanically Controlled Process (TMCP). FCA welding was performed using three kinds of welding consumables having the similar chemical composition including 0.04 wt.% C except for boron and manganese contents in the AWS Class. E81T1-K2C grade (A: 1.02% Mn - 42 ppm B, B: 1.02% Mn, - 1 ppm B, and C: 1.46% Mn - 2 ppm B).

Welding consumable B removed boron from welding consumable A, and welding consumable C increased manganese content in welding consumable B to 1.46 wt.%. Hot cracking and mechanical properties were evaluated according to the differences in boron and manganese content.

The hot crack resistance testing was performed with specimen having 400 mm wide and 600 mm long as shown in Fig. 1, and were subjected to grooving with a length of 400 mm and two

lamela. Dodavanje Mn u metal šava potisnulo je stvaranje feritnih lamela i povećalo je žilavost pri niskim temperaturama. Dakle, minimiziranjem količine B i dodavanjem Mn uspešno je povećana otpornost na tople prsline i žilavost na niskim temperaturama zavarenih spojeva ugljeničnih čelika visoke čvrstoće klase zatezne čvrstoće od 550 MPa.

1. Uvod

Tople prsline nastaju tokom ili neposredno posle zavarivanja kod mikrostruktura osetljivih na stvaranje prslina i zbog zateznih napona, usled skupljanja i spoljašnjih ograničenja zavarenog spoja. na temperaturama višim od 300 ℃

Glavni uzročnik stvaranja toplih prslina je niska rastvorljivost fosfora (P) i sumpora (S) u austenitnoj osnovi površinski orijentisanih kristalih struktura (FCC). Takođe, austenitni nerđajući i visokolegirani čelici kao što su legure nikla imaju nisku otpornost ka toplim prslinama [1].

Svrha ove studije je procena uticaja sadržaja bora (B) na otpornost na stvaranje toplih prslina elektrolučno zavarenih spojeva punjenim elektrodnim žicama (FCA) kod ugljeničnih čelika klase zatezne čvrstoće od 550 MPa. Posebno je ispitana promena mehaničkih osobina u odnosu na sadržaj bora kako bi se sprečile tople prsline, i prilagođavanje hemijskog sastava manganom (Mn) radi osiguranja mehaničkih osobina.

2. Materijali i eksperimentalni postupci

2.1 Osnovni metal i uslovi zavarivanja

Osnovni metal koji se koristi u ovoj studiji je ugljenični čelik visoke čvrstoće (klase: AH36) proizveden procesom Thermo Mechanical Controlled Process (TMCP). Elektrolučno zavarivanje punjenim elektrodnim žicama (FCA) je izvedeno upotrebom tri vrste materijala za zavarivanje sa 0,04 tež% C i različitim koncentracijama bora i mangana u AVS klasi. E81T1 -K2C razred (A: 1,02% Mn - 42 ppm B, B: 1,02% Mn, - 1 ppm B, i C: 1,46% Mn - 2 ppm B).

Upotrebljeni dodatni materijal za zavarivanje je B je sa uklonjenim borom iz materijala A, a upotrebljeni dodatni materijal za zavarivanje C imao je povećani sadržaj mangana u materijalu za zavarivanje B na 1,46 mas.%. Otpornost na tople prsline i mehanička svojstva ocenjivana su prema razlikama u sadržaju bora i mangana.

Ispitivanje otpornosti na tople prsline izvedeno je na uzorcima širine 400 mm i dužine 600 mm, kao što je prikazano na slici 1, i formirani su šavovi

conditions of low current (220 A) and high current (280 A) respectively.

dužine 400 mm, primenom niske (220 A) i visoke struje (280 A), respektivno.

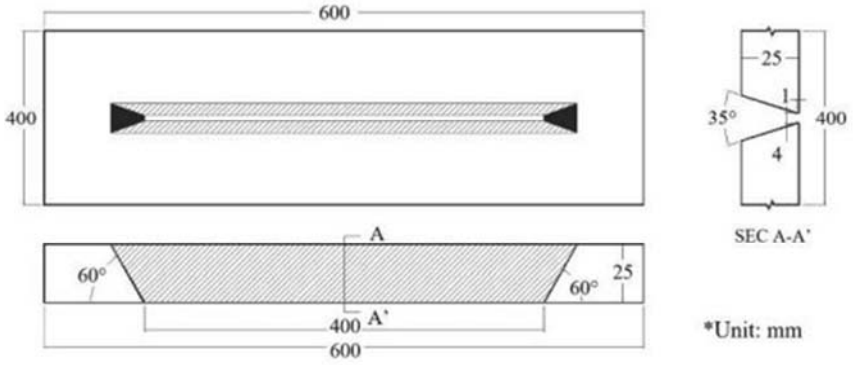

Figure 1. *Specimen geometry for hot crack resistance testing*

Slika 1. *Geometrija uzorka za ispitivanje otpornosti na tople prsline*

Further, additional specimens were prepared on the same base metal with the hot crack resistance testing specimen to confirm the change of mechanical properties according to the adjusted chemical composition.

Tab. 1 shows the bead sequence and detailed welding conditions for the evaluation of hot crack resistance and mechanical properties.

Dalje, dodatni uzorci su pripremljeni na istom osnovnom metalu sa uzorkom za ispitivanje otpornosti na tople prsline kako bi se potvrdila promena mehaničkih osobina u skladu sa prilagođenim hemijskim sastavom.

Tabela 1 prikazuje redosled i detaljne uslove zavarivanja radi procene otpornosti na tople prsline i mehaničkih osobina.

Table 1. *Welding conditions to check hot crack resistance and mechanical properties (Welding position: 1G*

Tabela 1. *Uslovi zavarivanja radi procene otpornosti na tople prsline i mehaničkie osobine (položaj zavarivanja: 1G)*

	Redosled zavarivanja	Uslovi zavarivanja				
		Prolaz Br.	Struja, (A)	Napon, (V)	Brzina kretanja (CPM)	Unos toplote, (kJ/cm)
Otpornost na tople prsline	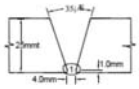	1	220	27	17,0	21.0
		1	280	31	24,8	21.0
Mehaničke osobine	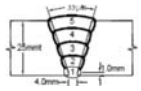	1	220	26	11,4	30.1
		2-5	300-330	32-34	19,2- 22,4	30.1

2.2 Hot crack resistance and mechanical testing

The specimens for the evaluation of hot crack resistance were subjected to liquid penetrant testing as shown in Fig. 2 to determine the crack length and the number of cracks visually confirmed.

Also, all weld metal tensile test, hardness test and impact test were carried out on the specimens for evaluation of mechanical properties. As shown in Fig. 3, the impact test was separated into root and face weld metal and carried out in 1 set of three specimens at each area.

2.2 Otpornost na tople prsline i ispitivanje mehaničkih osobina

Uzorci za procenu otpornosti na tople prsline podvrgnuti su ispitivanju penetrantima kao što je prikazano na slici 2, da bi se odredila dužina prslina i vizuelno potvrdio broj prslina.

Takođe, sva ispitivanja zatezanjem metala šava, ispitivanje tvrdoće i ispitivanje energije udara, izvršeno je radi procene mehaničkih svojstava. Kao što je prikazano na slici 3, ispitivanje enegije udara je razdvojeno na koren i lice metala šava i izvedeno je u setu od tri uzorka za svako područje.

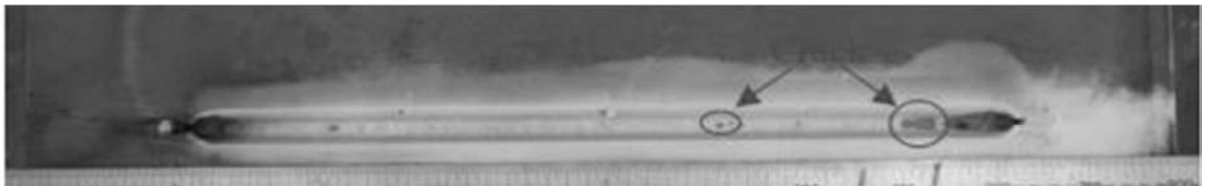

Figure 2. *Top surface of hot crack testing specimens after liquid penetrant testing*

Slika 2. *Lice šava uzoraka za ispitivanje na otpornost na tople prsline nakon ispitivanja penetrantima*

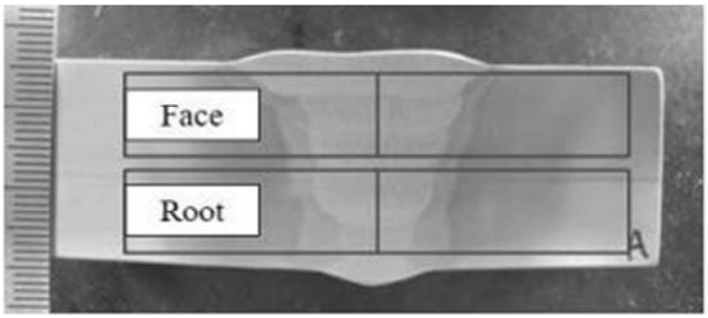

Figure 3. *Location of impact-testing specimens*

Slika 3. *Položaj uzoraka za ispitivanje energije udara*

2.3 Metallurgical analysis

The crack type was analyzed by Scanning Electron Microscopy (SEM) through analysis of fracture surface. Secondary ion mass spectrometry (SIMS) was used to analyze boron content added in small quantities in tens of ppm [2]. And, the specimens were prepared by Focused Ion Beam (FIB) and analyzed by Transmission Electron Microscopy (TEM).

Chemical compositions were analyzed by Optical Emission Spectroscopy (OES) in order to investigate the change of composition and mechanical properties for weld metal by dilution with base metal.

3. Results and discussion

3.1 Hot cracking behaviour by boron and manganese content

Fig. 4a and 4b show the results of the liquid penetrant testing at the low current (220 A) and high current (280 A) conditions respectively. The cracks for low current conditions were observed in the longitudinal direction of the weld line only for the welding consumable A having a boron content of 42 ppm. The cracks occurred in all welding consumables under high current conditions, but the total crack length was longest and the number of cracks was largest in case of welding consumable A having a boron content of 42 ppm. And, welding consumable B removed boron showed the shortest crack length and the smallest number of cracks under high current conditions.

2.3 Metalurška analiza

Tip prslina je analiziran skenirajućom elektronskom mikroskopijom (SEM) analizom površine loma. Sekundarna jonska masena spektrometrija (SIMS) korišćena je za analizu sadržaja Bora koji se dodaje u malim količinama, u desetinama ppm [2]. Uzorci su pripremljeni fokusiranim jonskim snopom (FIB) i analizirani transmisionom elektronskom mikroskopijom (TEM).

Hemijski sastavi su analizirani optičkom emisionom spektroskopijom (OES) kako bi se ispitala promena sastava i mehaničkih osobina metala šava razblaživanjem sa osnovnim metalom.

3. Rezultati i diskusija

3.1 Otpornost na tople prsline u zavisnosti od sadžaja bora i mangana

Na slikama 4a i 4b prikazani su rezultati ispitivanja penetrantima u uslovima niske (220 A) i visoke struje zavarivanja (280 A). Prsline nastale u uslovima niske struje su uočene u uzdužnom pravcu linije zavarivanja samo za materijal A sa sadržajem bora od 42 ppm. Do stvaranja prslina je došlo u svim dodatnim materijalima za zavarivanje u uslovima visokih struja, a ukupna dužina prsline bila najduža, a broj prslina najveći u slučaju dodatnog materijala za zavarivanje A sa sadržajem bora od 42 ppm. Dodatni materijal B je sa uklonjenim borom je pokazao najkraću dužinu prslina i najmanji broj prslina u uslovima visokih struja.

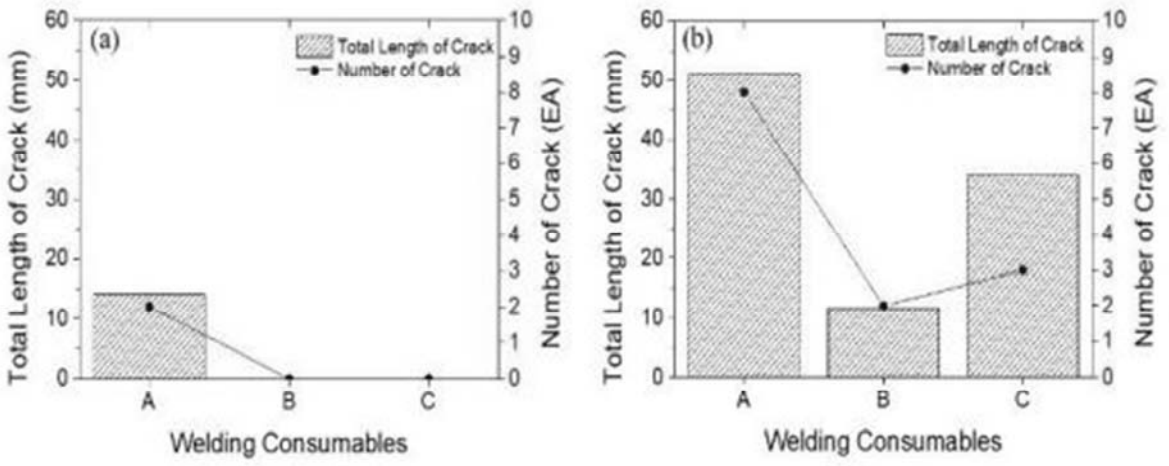

Figure 4. *Total crack length and number of cracks after liquid penetrant testing for the welds produced at (a) low current and (b) high current*

Slika 4. *Ukupna dužina prslina i njihov broj nakon ispitivanja pentrantima za zavarene spojeve proizvedene pri (a) niskoj i (b) visokoj struji.*

Fig. 5 is an optical microscope photograph for the cross section of the weld metal occurred cracking along the length of the weld line in the specimen welded at high current (280 A) with welding consumable A having high boron content.

Slika 5 je fotografija sa optičkog mikroskopa za poprečni presek šava gde je pucanje nastalo duž linija zvarivanja u uzorku zavarenom visokom strujom (280 A) sa dodatnim materijalom A sa visokim sadržajem bora.

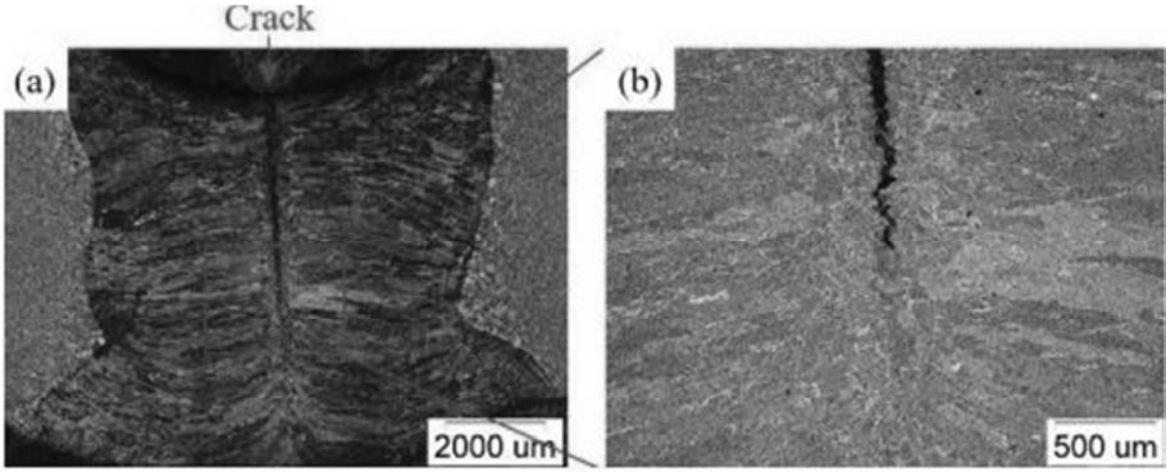

Figure 5. *Cross section of hot crack specimens produced by weld metal A and high current (280 A): (a) weld cross section and (b) enlarged view of hot crack observed in the weld centerline*

Slika 5. *Poprečni presek toplih prslina u uzoraku koji je zavaren dodatnim metalom A i visokom strujom (280 A): (a) presek vara i (b) uvećan prikaz tople prsline uočene u središnjoj liniji šava*

As shown in Fig. 5a, the crack was observed in the depth direction at the weld metal centerline, which is the final solidification point where the dendritic microstructures grown on the solid-liquid interface meet.

Kao što je prikazano na slici 5a, uočena je prslina u dubini središnje linije šava, što je poslednja tačka očvršćavanja gde se susreću dendritne mikrostrukture nastale na granici čvrsto/tečno.

Fig. 6 is a SEM image of the fracture surface for crack of the welded joint under the same condition. The liquid phase was solidified and the generated columnar dendrites were observed, which is judged to be typical hot cracking.

Slika 6. je SEM slika površine loma zavarenog pod istim uslovima. Tečna faza je očvrsnula i uočeni su stubasti dendriti, za koje je procenjeno da su tipični za tople prsline.

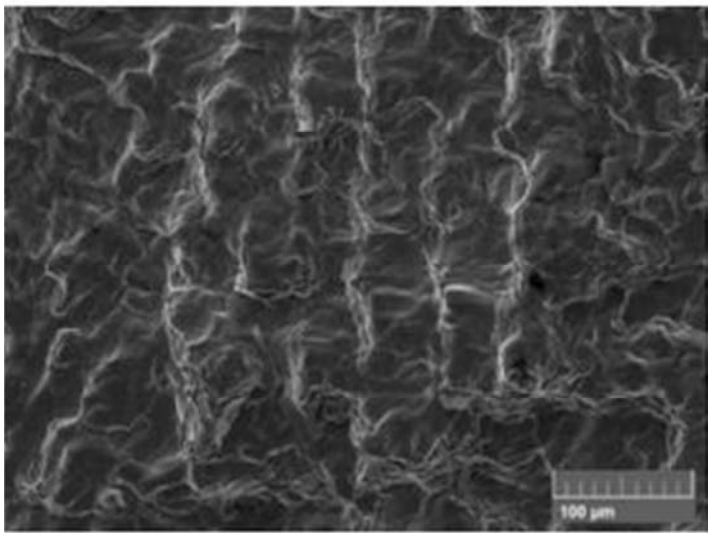

Figure 6. *SEM micrograph of fractured surface for the hot crack specimens produced by weld metal A and high current (280 A)*

Slika 6. *SEM mikrografija snimljene površine loma sa toplim prslinama kod uzoraka zavarenih dodatnim metalom A sa visokom strujom zavarivanja (280 A)*

3.2 Hot cracking mechanism by boron and manganese content

Fig. 7 is an SEM image of the microcracks directly connected to the end (Fig. 7a) and the side (Fig. 7b) of hot crack for welding consumable A, where only the hot crack occurred under the low current (220 A) condition. SIMS was performed for the chemical composition analysis at the position closest to the end of hot crack (Yellow square in Fig. 7a).

3.2 Mehanizam nasatajanja toplih prslina u zavisnosti od sadržaja bora i mangana

Slika 7 je SEM izgled mikropsline direktno povezane sa krajem (Slika 7a) i bočnom stranom (Slika 7b) tople prsline nastale zavarivanjem dodatnim materijalom A, gde je topla prslina nastala samo u uslovima niske struje (220 A). SIMS analiza hemijskog sastava je izvršena na položaju najbližem kraju tople prsline (svetli kvadrat na slici 7a).

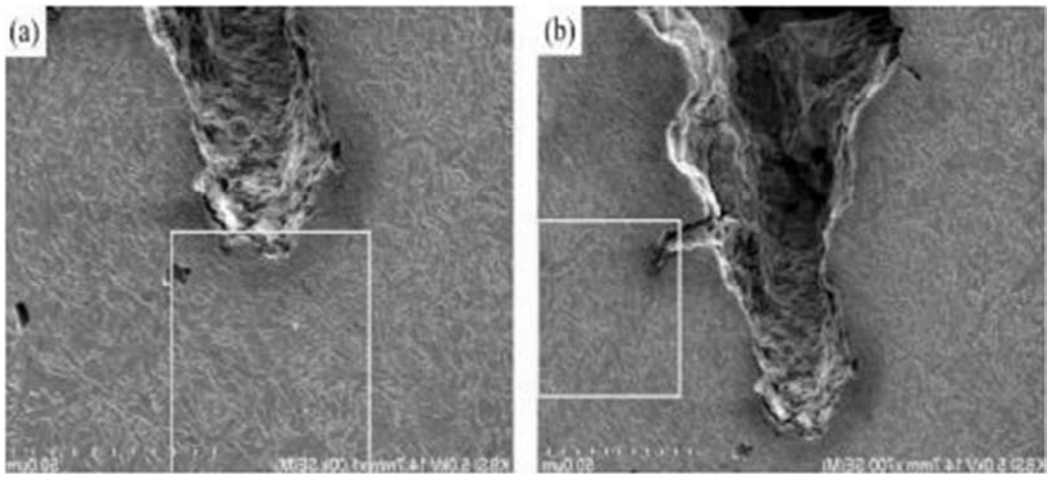

Figure 7. *Location of SIMS analysis for the hot crack produced by welding consumable A and low current (220 A): (a) the end of hot crack and (b) the side of hot crack*

Slika 7. *Položaj SIMS analize za toplu prslinu nastalu zavarivanjem dodatnim materijalom A niskom strujom (220 A): (a) kraj i (b) strana tole prsline*

Fig. 8 shows the mapping of boron, carbon, nitrogen and iron, and the results of line scan for the direction of 1 → 2 in mapping of boron and iron components. At the end of hot crack, boron (Fig. 8a) was concentrated and distributed around the

Slika 8. prikazuje mapiranje sadržaja bora, ugljenika, azota i željeza i rezultate linijskog skeniranja za pravac 1 → 2 za komponente bora i željeza. Bor (slika 8a) je koncentrovan na kraju tople prsline i raspoređen oko prsline. Ugljenik

crack. The carbon (Fig. 8b) and nitrogen (Fig. 8c) were also concentrated at the end of hot crack, similar to the position of boron, and segregated around the cracks. As a result of the line analysis, the degree of boron segregation was high at the end of hot crack, and iron showed uniform composition distribution.

Therefore, it is assumed that precipitates such as boron carbide ($Fe_{23}(C,B)_6$) formed by combining boron with carbon and iron or boron nitride (BN) produced by bonding with nitrogen are concentrated at the end of hot crack [3-5].

(slika 8b) i azot (slika 8c) su takođe segregirani oko prslina i koncentrisani na njihovim krajevima, slično položaju bora. Kao rezultat linijske analize, stepen segregacije bora bio je visok na kraju tople prsline, a železo je pokazalo ravnomernu raspodelu sastava.

Stoga se pretpostavlja da se talozi poput bor-karbida ($Fe_{23}(C, B)_6$) nastali spajanjem bora sa ugljenikom i železom ili bor - nitridom (BN) i da se koncentrišu na krajevima toplih prslina [3-5].

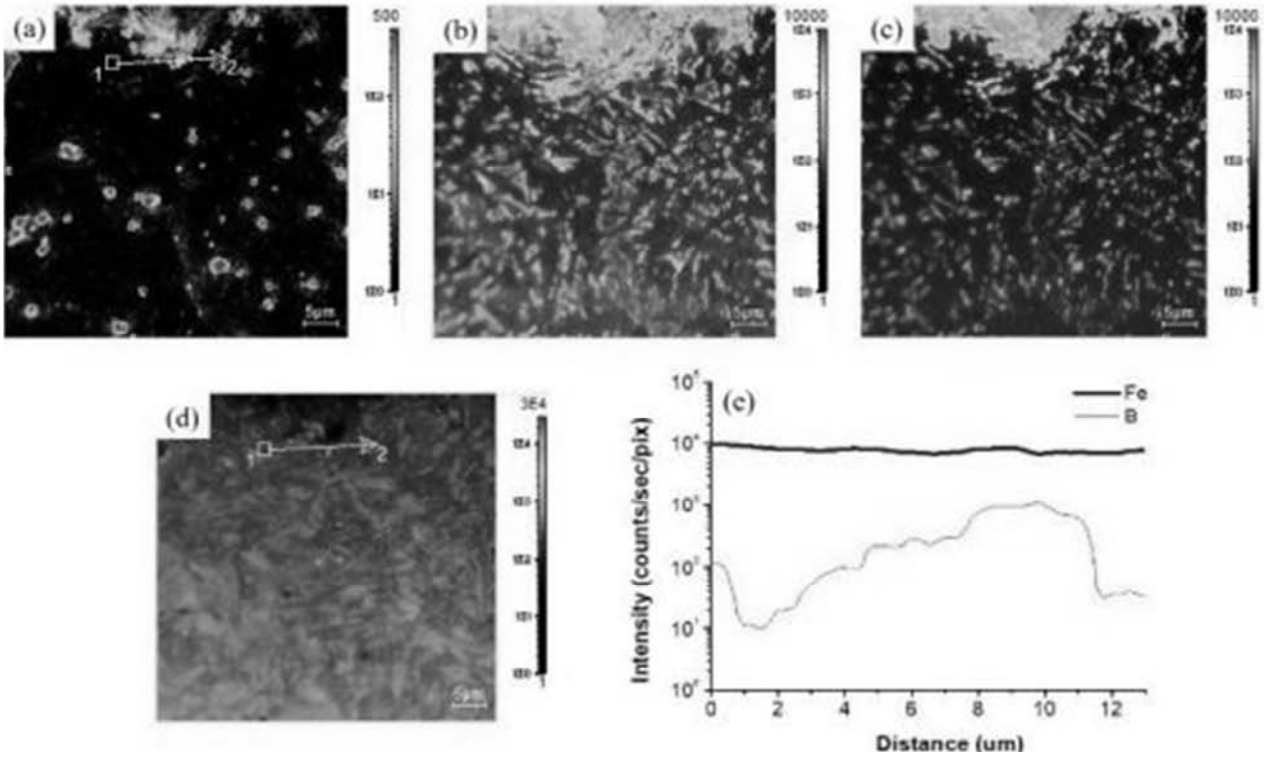

Figure 8. *Concentration maps measured by SIMS for the end of hot crack produced by welding consumable A and low current 220 A: (a) boron, (b) carbon, (c) nitrogen, (d) Fe elements and (e) line scan profiles starting from position 1 to 2 indicated in (a,d)*

Slika 8. *Mape koncentracije merene SIMS-om na kraju tople prsline nastale zavarivanjem dodatnim materijalom A, niskom strujom od 220 A: elementi (a) bor, (b) ugljenik, (c) azot, (d) Fe i (e) linijski profili skeniranja koji počinje od položaja 1 do položaja 2 naznačenih u (a, d)*

Based on the results of SIMS, a specimen for TEM analysis was prepared using FIB at the area (Red square in Fig. 9a) judged as precipitates in the grain boundaries closest to the microcrack at the side of hot crack to confirm the kind of precipitate formed by the combination of boron with other elements.

Fig. 9b-9d are the results of analysis of the respective TEM diffraction patterns at positions 1-3 of Fig. 9a, all of which are identified as $M_{23}C_6$ type carbides.

Na osnovu rezultata SIMS-a, uzorak za TEM analizu pripremljen je pomoću FIB-a na području (crni kvadrat na slici 9a) sa pretpostavkom da je talog u granicama zrna najbliži do mikroprsline na strani tople prsline da bi se potvrdilo da je ta vrsta taloga nastala kombinovanjem bora sa drugim elementima.

Slike 9b-9d prikazuju rezultate analize odgovarajućih obrazaca difrakcije TEM-a na pozicijama 1-3 na slici 9a, koji su svi identifikovani kao karbidi tipa $M_{23}C_6$.

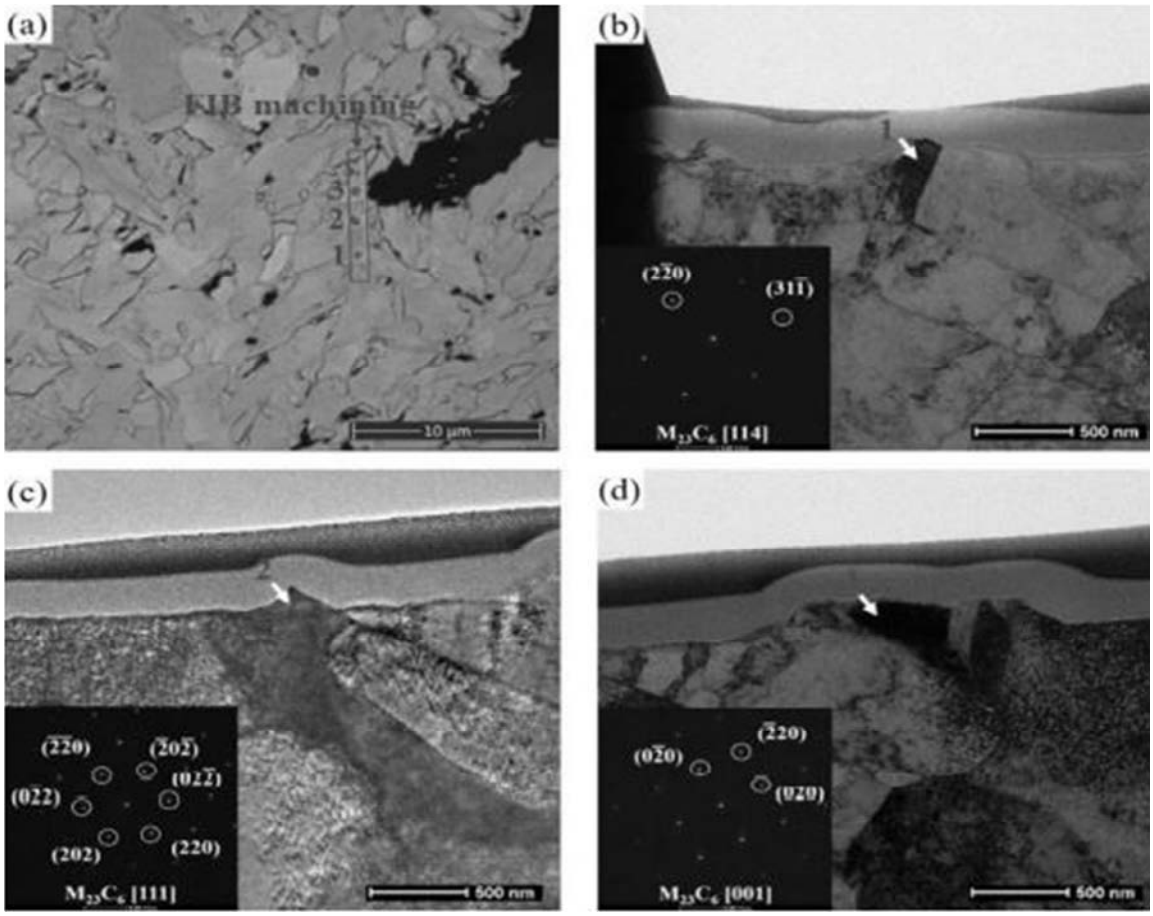

Figure 9. *TEM micrographs for the side of hot crack produced by welding consumable A and low current (220 A): (a) location of FIB machining, (b) bright field image and diffraction pattern for No. 1 precipitate, (c) bright field image and diffraction pattern for No. 2 precipitate and (d) bright field image and diffraction pattern for No. 3 precipitate*

Slika 9. *TEM mikrografije na strani tople prsline nastale zavarivanjem dodatnim materijalom A sa niskom strujom (220 A): (a) mesto FIB obrade, (b) slika svetlog polja i difrakcioni uzorak za talog br. 1, (c) slika svetlog polja i difrakcioni uzorak za talog br. 2 i (d) slika svetlog polja i difrakcioni obrazac za talog br. 3*

The results of the quantitative analysis by Energy Dispersive X-ray Spectroscopy (EDS) at the same position are as shown in Tab. 2. As a result of the atomic percent analysis, carbon and boron exist in the precipitates 1-3. Therefore, the precipitates are boron carbides ($Fe_{23}(C,B)_6$).

Rezultati kvantitativne analize pomoću energetsko disperzione rentgenske spektroskopije (EDS) u istoj tački su prikazani u Tabeli 2. Kao rezultat atomske procentualne analize, ugljenik i bor postoje u talozima 1-3. Zbog toga su to bor-karbidni talozi ($Fe_{23}(C, B)_6$).

Table 2. *Chemical composition of precipitates measured by TEM/EDS*

Tabela 2. *Hemijski sastav taloga meren pomoću TEM/EDS-a*

Br.	Sadržaj	Element				
		CK	Fe K	NK	BK	Ukupno
1	tež.%	3.2	95.7	0.0	1.1	100.0
	at.%	12.6	82.4	0.0	5.0	100.0
2	tež.%	1.8	97.2	0.0	1.0	100.0
	at.%	7.5	87.9	0.0	4.6	100.0
3	tež.%	1.9	97.1	0.1	0.9	100.0
	at.%	7.8	87.6	0.4	4.2	100.0

3.3 Mechanical properties and microstructure by boron and manganese contents

The tensile properties of the multi-layered welds according to the alloying elements are shown in Fig. 10a. Welding consumable A containing boron and welding consumable C having increased manganese content showed high yield and tensile strength and welding consumable B having a relatively low content of boron and manganese showed the lowest strength value. However, the welding consumables A-C satisfied both the minimum yield strength of 470 MPa and the tensile strength of 550-690 MPa required by the AWS Class E81T1-K2C of AWS A5.29.

Fig. 10b shows the Vickers hardness values for the weld metals as the minimum and maximum values. All of the welding consumables have a hardness lower than the maximum 350 HV10 required by the Society and satisfy acceptance criteria. The hardness value of the welding consumable C having a high manganese content is about 20 HV10 higher than the welding consumables A and B.

The hardness of welding consumable C is considered to be the highest because of the effect of increasing hardenability with increasing manganese content when comparing welding consumables B and C having the same chemical composition except for manganese.

3.3 Mehanička svojstva i mikrostrukture u zavisnosti od sadržaju bora i mangana

Zatezne karakteristike višeprolaznih varova na osnovu legirajućih elemenata prikazane su na Slici 10a. Dodatni materijal A koji sadrži bor i materijal C sa povećanim sadržajem mangana pokazali su visoke vrednosti za granicu tečenja i zateznu čvrstoću. Dodatni materijal B sa relativno niskim sadržajem bora i mangana pokazao je najnižu vrednost čvrstoće. Međutim, dodatni materijali A-C su zadovoljili oba zahtevana kriterijuma za klasu E81T1-K2C iz grupe AWS A5.29, i minimalnu granicu tečenja od 470 MPa i zateznu čvrstoću od 550-690 MPa.

Slika 10b prikazuje vrednosti Vickers-ove tvrdoće za zavarene spojeve kao minimalne i maksimalne vrednosti. Svi dodatni materijali za zavarivanje imaju tvrdoću manju od zahtevanih maksimalnih 350 HV10 i zadovoljavaju kriterijume prihvatljivosti. Vrednost tvrdoće dodatnog materijala za zavarivanje C sa visokim sadržajem mangana je za oko 20 HV10 veća od materijala A i B.

Kada se porede dodatni materijali B i C koji imaju isti hemijski sastav osim mangana, smatra se da je tvrdoća materijala C veća zbog efekta povećanja čvrstoće sa povećanjem sadržaja mangana.

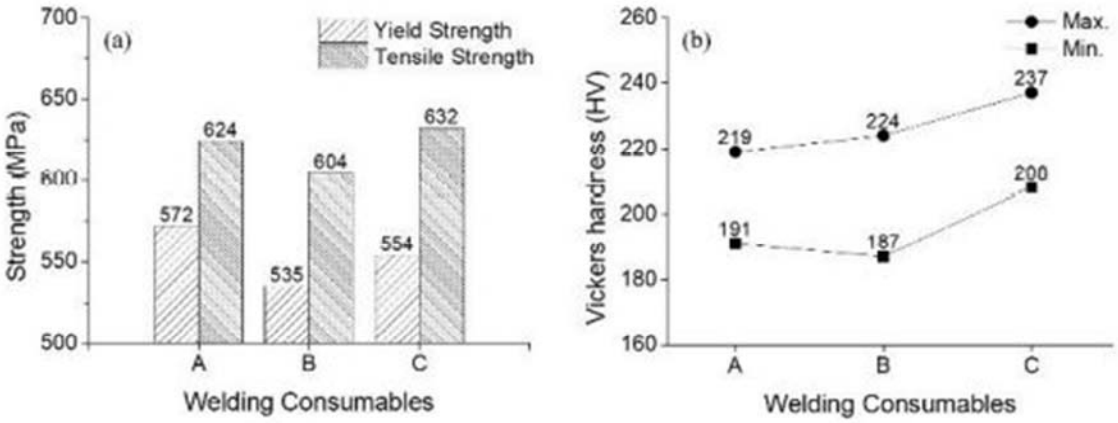

Figure 10. *Mechanical properties for the welds produced by various welding consumables: (a) yield and tensile strengths and (b) Vickers hardness*

Slika 10. *Mehanička svojstva zavarenih spojeva koji su zavareni različitim dodatnim materijalima za: (a) granica tečenja i zatezna čvrstoća i (b) Vickers -ova tvrdoća*

Fig. 11 shows the impact test results measured at -20 ℃for each welding consumable. The impact test results of the face weld metal showed good impact value of 98 J or more in all the welding consumables, but the welding consumable B had a

Slika 11. prikazuje rezultate ispitivanja energije udara merenih na -20 ℃ za svaki dodatni materijal. Rezultati ispitivanja energije udara sa lica metala šava pokazali su dobru vrednost energije udara od 98 J ili više kod svih dodatnih materijala, ali je materijal B imao veliko odstupanje sa

large deviation with a minimum value of 85 J and a maximum value of 112 J.

In addition, the impact test results for the root weld metal showed the lowest value of average 22 J for welding consumable B compared to welding consumable A and C.

minimalnom vrednošću od 85 J i maksimalnom vrednošću od 112 J.

Osim toga, rezultati ispitivanja energije udara korena metala šava pokazali su najnižu vrednost od prosečno 22 J za dodatni materijal B u poređenju sa materijalom A i C.

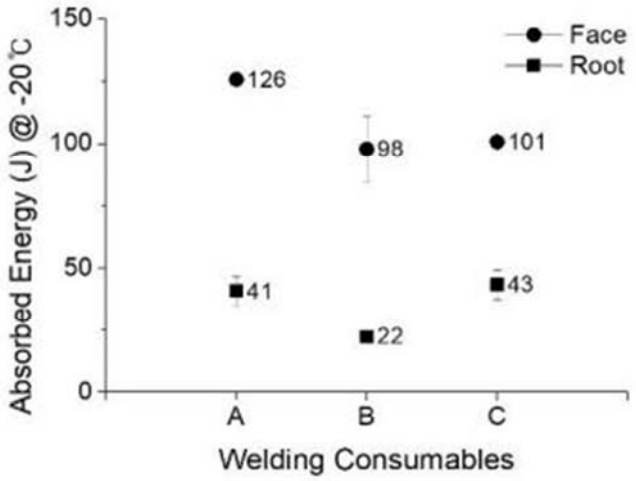

Figure 11. *Impact toughness measured at -20 ℃ for various welding consumables*

Slika 11. *Energija udara merena pri -20 ℃ za različite dodatne materijale*

Chemical compositions were analyzed to determine the causes of low toughness at low temperature on the root weld metal. The results are shown in Tab. 3.

The carbon content of the welding consumables was 0.04 wt.%, but the carbon content of the weld metal increased to 0.07-0.08 wt.% by dilution with the base metal. The boron content of the weld metal A was similar to that of the welding consumable A. The boron content of the weld metal B and C was higher than that of the welding consumables but the boron content was considerably lower than that of the weld metal A. The manganese content of the weld metals remained similar to the chemical composition of the welding consumables.

Hemijski sastavi su analizirani da bi se utvrdili uzroci niske žilavosti pri niskim temperaturama u korenu zavarenog spoja. Rezultati su prikazani u Tabeli 3.

Sadržaj ugljenika u dodatnom materijalu je bio 0,04 tež.% ali je sadržaj ugljenika povećan na 0,07-0,08 tež. % usled mešanja sa osnovnim metalom. Sadržaj bora u metalu šava koji je zavaren dodatnim materijalom A bio je sličan sadržaju samog dodatnog materijala A. Sadržaj bora u metalu šava B i C bio je veći od sadržaja u dodatnom materijalu, ali je sadržaj bora bio znatno niži nego u metalu šava kod A. Sadržaj mangana u metalima šavova je ostao sličan hemijskom sastavu dodatnih materijala.

Table 3*. Chemical composition of root weld metal (wt.%)*

Tabela 3. *Hemijski sastav korena metala šava (tež.%)*

ID	C	Si	Mn	P	S	Ti	B
A, ppm	0,07	0,40	1,03	0,013	0,006	0,06	46
B, ppm	0,08	0,45	1,07	0,013	0,006	0,06	8
C, ppm	0,08	0,44	1,44	0,013	0,006	0,06	10

Fig. 12 is a representative microstructure analyzed by optical microscope (OM) on the root weld metal. Welding cosumable A and C were

Slika 12. je tipična mikrostruktura analizirana optičkim mikroskopom (OM) korena šava. Dodatni materijali A i C su se uglavnom sastojali od mainly

composed of acicular ferrite (AF) and grain boundary ferrite (GBF). However, in the welding consumable B, not only AF and GBF but also ferrite side plates (FSP) were observed.

igličastog ferita (AF) i ferita na granici zrna (GBF). Međutim, u dodatnom materijalu B, nisu primećene samo AF i GBF već i feritne lamele (FSP).

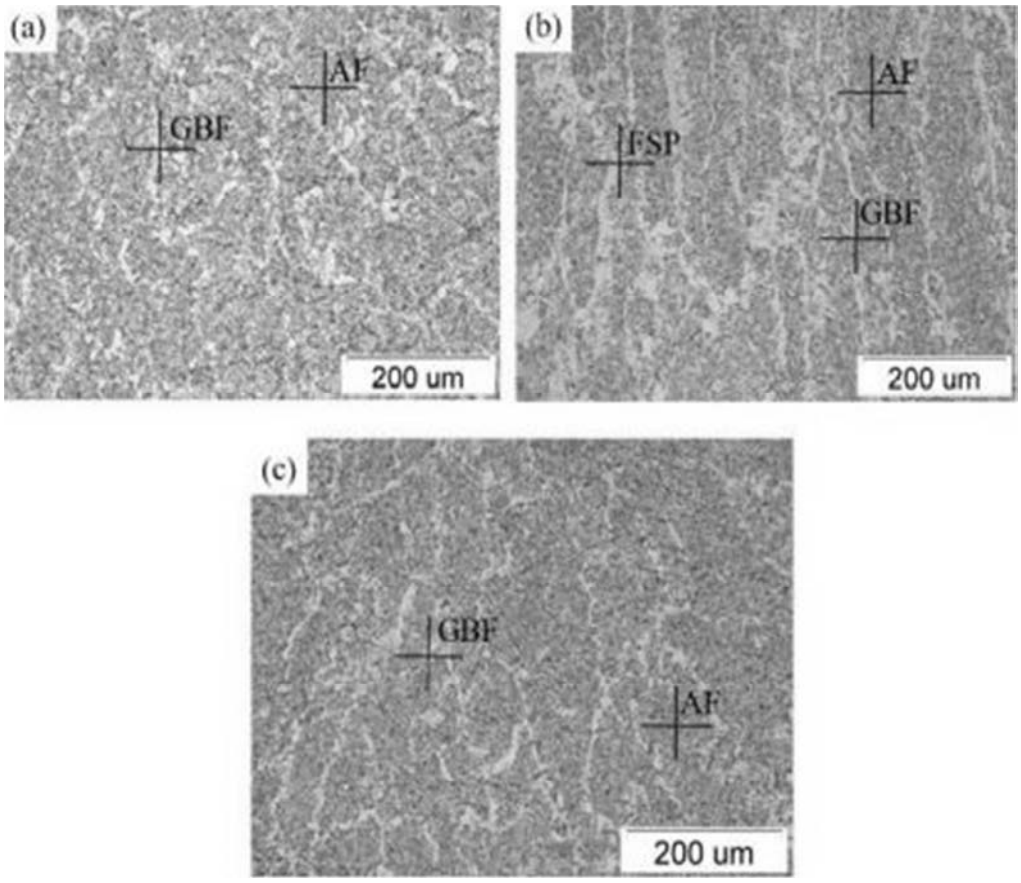

Figure 12. *Microstructure for root weld metal produced from various welding consumables: (a) ID-A, (b) ID-B, (c) ID-C (GBF : Grain Boundary Ferrite, AF : Acicular Ferrite, FSP : Ferrite Side Plate)*

Slika 12. *Mikrostruktura korena metala šava formirana različitim materijalima za zavarivanje: (a) ID-A, (b) ID-B, (c) ID-C (GBF: Ferit na granici zrna, AF: Igličasti ferit, FSP: lamelarni ferit)*

Fig. 13 is a representative microstructure analyzed by OM and SEM on the face weld metal. The face weld metal is a microstructure for the final weld bead that is not affected by reheating from the subsequent weld pass relative to the microstructure of the root weld metal.

Welding consumable B was relatively large in size of FSP and produced a large amount of FSP. The results of impact test at the low temperature for the face weld metal can be explained by more AF and few GBF and FSP on the microstructure of welding consumable A than the welding consumable C. In addition, the SEM image of high magnification for the face weld metal as shown in Fig. 13d-13f can easily distinguish that the size of the GBF for the welding consumable B is larger than that of the welding consumable A and C.

Slika 13. je tipična mikrostruktura analizirana OM-om i SEM-om na licu metala šava. Metal lica šava je mikrostruktura za završni prolaz na koji ne utiče ponovno zagrevanje u odnosu na mikrostrukturu korenog dela metala šava.

Dodatni materijal B je imalo veliku količinu lamelarnog ferita i relativno krupne lamele ferita. Rezultati ispitivanja energije udara na niskoj temperaturi metala lica šava mogu se objasniti sa većom količinom igličastog ferita, nešto ferita na granici zrna i lamelarnog ferita u mikrostrukturi dodatnog materijala A nego kod dodatnog materijala C. Osim toga, sa SEM slika pri velikom uvećanja lica metala šava, kao što je prikazano na slikama 13d-13f, lako se može uočiti da je veličina GBF-a kod dodatnog materijala B veća nego kod dodatnih materijala A i C.

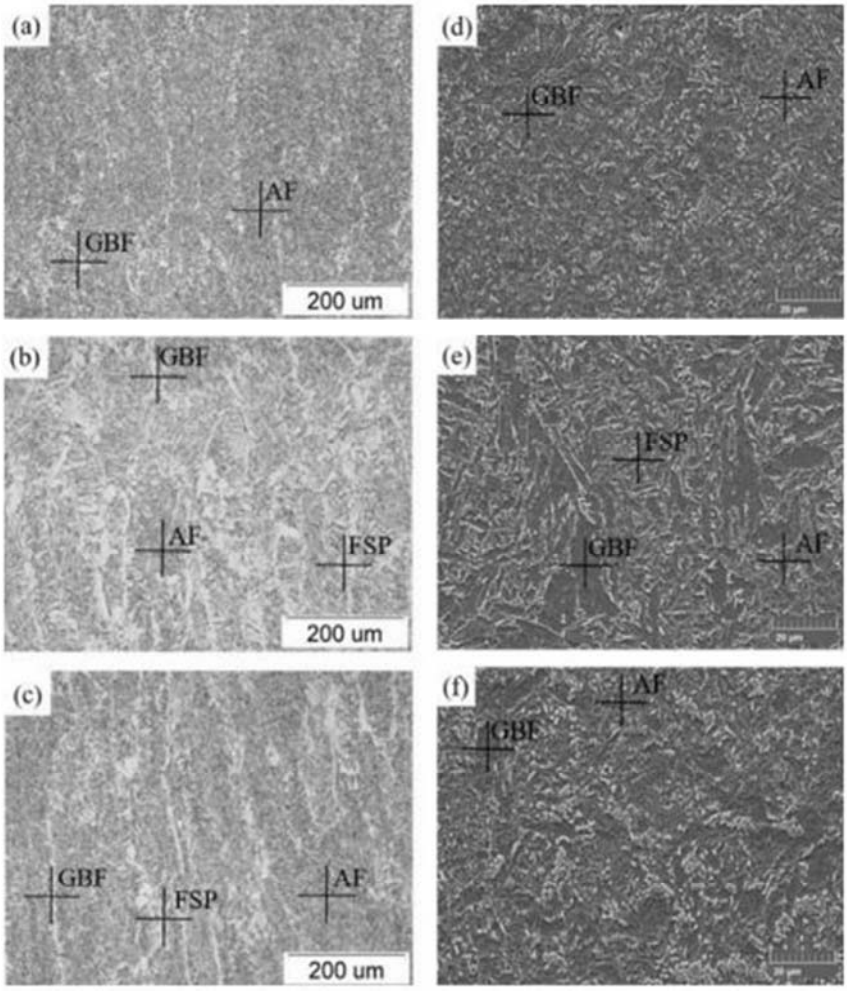

Figure 13. *Microstructure for face weld metal produced from various welding consumables: (a) OM image for ID-A, (b) OM image for ID-B, (c) OM image for ID-C, (d) SEM image for ID-A, (e) SEM image for ID-B and (f) SEM image for ID-C*

Slika 13. *Mikrostruktura lica metala šava formirana različitim dodatnim materijalima: (a) OM slika za ID-A, (b) OM slika za ID-B, (c) OM slika za ID-C, (d) SEM slika za ID-A, (e) SEM slika za ID-B i (f) SEM slika za ID-C*

Therefore, the welding consumable B having a reduced boron content in order to reduce the hot cracking has unstable impact toughness in the face weld metal and has low impact toughness in the root weld metal. This problem can be solved by the increase of manganese content because it accelerates AF formation and inhibits FSP formation, and supplement impact toughness of welding consumable C [6].

Stoga, dodatni materijal B u kojem je smanjen sadržaj bora radi umanjenja toplih prslina ima nestabilnu udarnu žilavost na licu metala šava i ima nisku udarnu žilavost u korenu šava. Ovaj problem se može rešiti povećanjem sadržaja mangana jer to ubrzava stvaranje igličastog ferita i inhibira stvaranje lamelarnog ferita i povećava udarnu žilavost dodatnog materijala C [6].

4. Conclusions

In order to investigate the effect of boron and manganese on the hot crack resistance and low temperature impact toughness of FCA weld metal for high strength carbon steel, the self-restraint test after single pass welding and mechanical properties and microstructure after multi-layer welding were analyzed and the following conclusions were obtained.

4. Zaključci

U cilju ispitivanja uticaja bora i mangana na otpornost na stvaranje toplih prslina i niskotemperaturnu udarnu žilavost elektrolučno zavarenih spojeva ugljeničnih čelika visoke čvrstoće sa punjenim elektrodnim žicama (FCA), vršeni su jednoprolazni testovi zavarljivosti, a mehaničke osobine i mikrostrukture nakon više prolaznih zavarivanja su analizirane i dobijeni su sledeći zaključci.

In the self-restraint test, FCA weld metal by welding consumable B and C with reduced boron content did not undergo hot cracking under low current (220 A) and low speed (17.0 CPM) welding conditions. However, hot cracking occurred at high current (280 A) and high speed (24.8 CPM) welding conditions even when boron-reduced welding consumables were used, and the length and number of hot cracks decreased compared to welding consuamble A with high boron content.

The hot cracking propagated along the grain boundaries of the weld centerline where the liquid phase finally existed during solidification.

According to SIMS analysis, the boron concentration around the hot crack was confirmed. It was found through TEM analysis that boron was bound to iron and carbon in the process of cooling at high temperature and existed as a precipitate of Fe23(C,B)6 in grain boundaries at room temperature.

Welding consumable B with reduced boron content was increased in nonuniformity according to low temperature impact value due to FSP growth. Welding consumable C with increased manganese content was able to secure low temperature toughness by suppressing FSP formation.

The high strength carbon steel welds of 550 MPa-grade tensile strength prevent hot cracking through minimization of boron content and secured low temperature toughness by increase of manganese content at the same time.

Kod testova zavarljivosti, u metalu šava koji je dobijen dodatnim materijalima B i C koji su imali smanjeni sadržaj bora, nisu otkrivene tople prsline pri niskim strujama (220 A) i niskim brzinama zavarivanja (17,0 CPM). Međutim, došlo je do pojave toplih prslina pri visokim strujama (280 A) i velikim brzinama zavarivanja (24,8 CPM), čak i kada su korišćeni dodatni materijali za zavarivanje sa smanjenom količinom bora. Dužina i broj toplih prslina je manji nego kada se koristio dodatni materijal A sa visokim sadržajem bora.

Tople prsline su se širile duž granica zrna centralne linije spoja gde tečna faza poslednja očvrććava.

Prema SIMS analizi, potvrđena je koncentracija bora oko toplih prslina. TEM analizom je utvrđeno da se bor vezao za železo i ugljenik tokom procesa hlađenja sa visokih temperatura i na sobnoj temperaturi se izdvojio kao talog Fe23(C,B)6 na granicama zrna.

Usled rasta lamelarnog ferita i na osnovu niskotemperaturne udarne žilavosti, dodatni materijal B sa smanjenim sadržajem bora, ima uvećanu neujednačenost osobina. Dodatni materijal C sa povećanim sadržajem mangana je obezbedio niskotemperaturnu žilavost suzbijanjem stvaranja lamelarnog ferita.

Kod zavarenih spojeva od ugljeničnog čelika visoke zatezne čvrstoće od 550 MPa, sprečavanje pojave toplih prslina postiže se minimiziranjem sadržaja bora, a u isto vreme obezbeđuje se niskotemperaturna žilavost povećanjem sadržaja mangana.

References / Literatura

[1] S. Kou, Welding Metallurgy, 2nd ed., pp. 279-280, John Wiley & Sons, New Jersey (2003).

[2] H. U. Hong, I. S. Kim, B. G. Choi, Y. S. Yoo and C. Y. Jo, Met. Mater. Trans. 43, 173 (2012).

[3] H. Tamehiro, M. Murata, R. Habu and M. Nagumo, Trans. ISIJ 27, 128 (1987)

[4] Y. S. Choi, S.J. Kim, I. M. Park, K. W. Kwon and I. S. Yoo, Met. Mater. 3, 121 (1997).

[5] D. J. Mun, E. J. Shin, Y. W. Choi, J. S. Lee and Y. M. Koo, Mater. Sci. Eng. A 545, 224 (2012).

[6] Z. Zhang and R. A. Farrar, Weld. J. 77, 195-s (1997).

Nastavak sa strane 100

68. GODIŠNJA SKUPŠTINA DRUŠTVA ZA UNAPREĐIVANJE ZAVARIVANJA U SRBIJI Beograd, 29.06.2021.

Predloženo je da se u časopisu objavi spisak tehničkih komisija IIW-a, kako bi članovi mogli da vide koje sve komisije postoje i čime se bave.

Spisak tehničkih komisija IIW-a je u nastavku:

Komisija br. C -	Naziv
I	Additive Manufacturing, Thermal Cutting and Allied Processes
II	Arc Welding and Filler Metals
III	Resistance welding, Solid State Welding and Allied Joining Processes
IV	Power Beam Processes
V	Non-Destructive Control and Quality Assurance of Welded Products
VI	Terminology
VII	Microjoining and Nanojoining
VIII	Health, Safety and Environment
IX	Behaviour of Metals Subjected to Welding
X	Structural Performances of Welded Joints - Fracture Avoidance
XI	Pressure Vessels, Boilers and Pipelines
XII	Arc Welding Processes and Production Systems
XIII	Fatigue Behaviour of Welded Components and Structures
XIV	Education and Training
XV	Design, Analysis and Fabrication of Welded Structures
XVI	Polymer Joining and Adhesive Technology
XVII	Brazing, Soldering and Diffusion Bonding
XVIII	Quality Management in Welding and Allied Processes

Martin Petreski [1, a], Dobre Runchev [1, b], Gligorche Vrtanoski [1, c]

Hybrid laser arc welding – state of the art in technology

Hibridno lasersko elektrolučno zavarivanje – pregled stanja tehnologije

Stručni rad / Professional paper
UDK / UDC: 621.791.725/.752

Rad primljen / Paper received:
Septembar 2021.

Adresa autora / Author's address:

[1]University „Ss. Cyril and Methodius“, Faculty of Mechanical Engineering, Karposh II bb, 1000 Skopje, Republic of North Macedonia

[a]martin.petreski@mf.edu.mk,

[b]dobre.runchev@mf.edu.mk,

[c]gligorche.vrtanoski@mf.edu.mk

Keywords: hybrid welding, laser beam, arc welding, welding parameters, applications

Ključne reči: hibridno zavarivanje, laserski snop, električni luk, parametri režima zavarivanja

Abstract

Hybrid laser arc welding is complex process where two heat sources act simultaneously in a common weld pool. The synergy effect of laser beam and electric arc offers several advantages over other individual technological processes, such as: higher welding speed, increased productivity, deeper penetration, better gap bridging ability, stable process, less heat input to the welding material, etc. However, the combination of two heat sources in a single welding process leads to large number of parameters that need to be synchronized and optimized in order to obtain a perfect weld. This paper presents the current state of hybrid laser arc welding in terms of its development, industrial application and scientific research. The introduction part contains a general overview of the hybrid laser arc welding process, its advantages and operating principles, and chronological development. In the second part, welding parameters that directly influence on the hybrid process have been discussed. The third part presents the performance and weld qualities achieved by hybrid welding process in accordance with previous research. In the final part, examples of industrial application and conclusions for further research and development related to hybrid laser arc welding are given.

Rezime

Hibridno zavarivanje sa laserskim snopom i električnim lukom je kompleksan proces gde dva izvora toplote istovremeno utiču na istom mestu na radnom materijalu. Efekat spajanja laserskog snopa i električnog luka nudi velike prednosti u odnosu na ostale individualne tehnološke procese, kao na primer: veće brzine zavarivanja, povećanu produktivnost i penetraciju, bolju popunu žlebova, stabilan proces, manje termičko opterećenje radnog materijala itd. Međutim, spajanje dva izvora toplote u jednom procesu zavarivanja vodi do povećanog broja parametara koji bi trebalo da se sinhronizuju i optimizuju u cilju dobijanja kvalitetnog zavarenog spoja. U ovom radu predstavljeno je trenutno stanje hibridnog zavarivanja sa laserskim snopom i električnim lukom u odnosu na njegov razvoj, industrijsku primenu i eksperimentalna istraživanja. Uvodni deo sadrži opšti pregled hibridnog procesa zavarivanja, njegove prednosti i principe rada, kao i hronološki razvoj. U sledećem delu detaljno su objašnjeni parametri koji direktno utiču na stabilnost hibridnog procesa. Dalje, predstavljene su performanse i kvalitet zavarenih spojeva dobijenih hibridnim procesom zavarivanja, a u skladu sa prethodnim istraživanja. Na kraju dati su primeri praktične primene hibridnog zavarivanja kao i predlozi za dalja istraživanja i razvoj.

1. Introduction

Today's globalization is characterized by an accelerated process movements of capital, resources, products and services, resulting in a completely new world trade structure, economic and financial flows, internationalization of production and acceleration of technical and technological development. As a part of mechnical engineering, the welding have not been lagging in technological development, new welding techniques and technologies are constantly being introduced, which would result in reduced production costs and improved technical characteristics of the welded joints [1].

The conventional joining process Gas Metal Arc Welding – GMAW is widely used process for welding of strucutural steel in a number of engineering fields such as shipbuilding, civil construction, mining equipment and metallurgy [2]. Consequently, several innovations appear in this welding process, that contributes for its improvement [3]. One of the improvements is automated hybrid laser arc welding, whereby combining the advantages of two different processes, Laser Beam Welding – LBW and semi-automatic welding processes such as Gas Metal Arc Welding – GMAW and Flux-Cored Arc Welding – FCAW represents an excellent substitute for conventional welding processes [4].

Even though GMAW is widely used welding process due to its advantages such as simple handling, relatively low cost for implementation, ability to bridge large root openings, welds with large cross sections and high deposition rate, the welding speed of GMAW is limited by the formation of defects [5]. In addition, during the welding process GMAW applies a high heat input to the welding material, resulting in large heat-affected zones HAZs and occurrence of the undesired microstructure [6]. On the other hand, LBW provides deep and narrow welds at high welding speeds, due to its high energy density, leading to a small HAZ and low distortion [7]. However, the LBW process like any other process has disadvantages, one of them is high cooling rate from the welding zone that leads to high weld metal hardness and low toughness, which sometimes cannot meet the minimum mechanical properties [8].

Hybrid Laser Arc Welding – HLAW combines the advantages of both welding processes, LBW and GMAW or FCAW, resulting in welding process that is characterized with high welding speed [9], low heat input, high penetration depth into the welding material, and the possibility of controlling the chemical composition of the weld bead [10].

For the first time, the hybrid laser arc welding process was introduced in the late 1970s by Prof. W. M. Steen [11], and the process was defined as “arc-augmented laser welding”. The results of its research showed a clear advantage of combining an electric arc and a laser beam for welding. Despite of the successful demonstration, hybrid welding’s further research and development experienced a slow growth due to lack of reliable laser source with high power, required human skills, and incomplete knowledge of the process [12]. In the late 1980s, the development of reliable and consistent high power industrial lasers, the researchers' attention was focused on improving the HLAW process for its application in everyday production [13]. Several drawbacks of the individual welding processes have been eliminated, such as gap bridging ability and reflectivity of the materials which were issues for successful welding [14]. In the 1990s, hybrid laser arc welding had acquired considerable developments due to availability of high-power CO2 lasers, where a mixture of CO_2:He:N_2 was used as the active medium [15, 16].

The first industrial hybrid laser arc welding system was introduced in 2000 by Fraunhofer ILT, Germany, in an oil tank manufacturing industry [17]. Later, this system has been installed in several industries including shipbuilding, steel tube manufacturing and automotive industries, etc. In 2001, the world-famous welding company Fronius introduced hybrid laser arc welding system with a compact laser hybrid head to a standard industrial robot, which integrated MIG/MAG welding torch and laser optics, figure 1 [16, 95].

Nowadays, plenty of hybrid laser arc welding systems are commercially available in the industry. The quantity of these systems has increased in the last decade not only as a result of commercially available integrated hybrid welding heads development, but also due to more cost-effective powerful lasers with advanced automated control [18].

Besides hybrid welding of laser beam and arc welding, today there is also available hybrid welding with combination of laser beam and plasma arc or submerged arc welding – SAW [16].

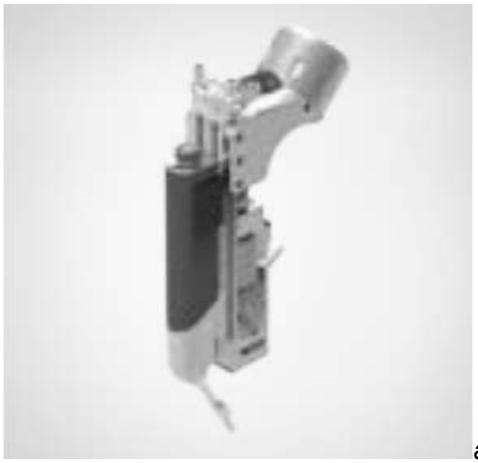
a)

b)

Figure 1. *a) Compact, b) Ultracompact – integrated welding head [16, 95]*

Slika 1. *a) Kompaktna, b) Ultrakompaktna – integrisana zavarivačka glava [16, 95]*

Furthermore, HLAW compensates the limitations of the individual LBW and GMAW processes, reducing the cooling rates from the weld zone and increasing the dimensional tolerances of the joints in comparison to LBW [20]. Additionally, HLAW offers several process advantages, such as: higher welding speed [21], requirement of fewer number of welding passes [22], increased penetration depth [23], narrow weld seam with small heat affected zones HAZs [24] and stable welding process [25].

The use of secondary heat source, as electric arc, compensates the requirement of high-power laser, thus directly affecting the cost of the set-up [21]. Hybrid laser arc welding process due to its advantages compared to other welding processes allows wide application in many industries, starting from the automotive to heavy metal industries [26], while welding different steels with thickness range from 1mm to 50mm [27].

Although the hybrid laser arc welding process has numerous process advantages, the process has certain limitations too, such as: controlling large numbers of process welding parameters, requirement of accurate positioning and proper fit-up of the welding material, higher initial investment, and additional safety measures. Consequently, HLAW is a complex welding process due to the combination of two heat sources in a single weld pool [28], resulting in non-acceptance by the industry [29].

2. Hybrid welding with laser beam and electric arc – HLAW

In the last decade, the development of the hybrid laser arc welding has been characterized by improvements of the welding technique where the laser beam and the electric arc act on the welding material at the same time and in the same place.

Several hybrid laser arc welding systems have been developed based on different combinations of laser beam and arc welding systems. The most commonly used lasers are gas CO2 lasers with continuous wave or Nd:YAG lasers with pulsed operation, while the second sources is electric arc MIG/MAG or TIG depending on the type and thickness of the welded material.

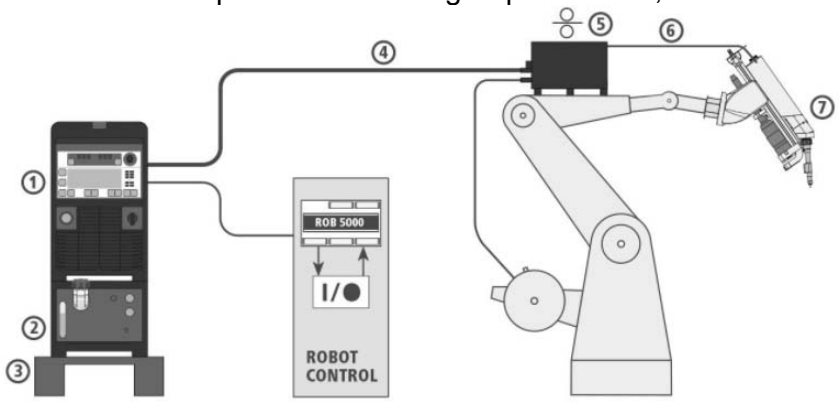

1. TransPuls Synergic
2. Cooling unit
3. Upright console
4. Interconnecting hosepack
5. Robot wirefeeder
6. Torch hosepack
7. LaserHybrid welding head

Figure 2. *System components of hybrid laser arc welding [95]*

Slika 2. *Komponente hibridnog sistema lasersko elektrolučnog zavarivanja [95]*

Although HLAW offers significant advantages over the individual LBW and GMAW processes, merger of the two heat sources in a single welding process leads to increased number of parameters that need to be synchronized. Moreover, the values of the parameters that are ideal for each process separately, are likely not to be optimal for successful welding with HLAW due to mutual influence. Consequently, an accurate study [30] of all the parameters used in the hybrid welding process is the basis for the stability and repeatability of the process and obtaining a weld with excellent mechanical and dimensional characteristics.

Usually, the lasers types that are used as a primary heat source in hybrid laser arc welding are gas CO_2 laser or solid state Nd:YAG laser that generate different wavelengths. The laser beam wavelength is the main welding parameter of HLAW, due to the direct influence on the choice of other welding parameters [31]. The type of laser source affects the distance between the both sources, Nd:YAG laser allows closer access to the electric arc compared to CO_2 laser due to a lower interaction with the electric arc [32].

In laser beam welding, the increase of laser power leads to deeper weld penetration [34]. In hybrid laser welding this phenomenon is often emphasized because the reflectivity of the workpiece metal is reduced when the metal is heated by the arc [35]. The hybrid laser arc welding process provides two different layouts for the heat sources. First layout is when the laser source is the first source that heats the working material - laser leading hybrid process. The second layout or arc leading hybrid process is when the electric arc is the first heat source that "attack" [36]. The layout depends on several factors, such as the characteristics of the welding material, the power of the laser beam and the electric arc [37].

The distance between the laser source and the arc is an important parameter to control the penetration in hybrid laser arc welding and normally is consisted of few millimeters value, separation distance is in the range of 0 to 5 mm [38]. Increasing the distance between the heat sources might result in loss of hybridization effects, i.e.to reduce the interaction between the laser beam and the electric arc [39]. When heat sources are placed in parallel or at a very short distance might lead to a problem of absorption of the laser energy by the electric arc, which partially blocks the laser beam resulting in less penetration [38, 40].

Another parameter in HLAW that directly affects the depth of the weld, but also the stability of the arc [41], and thus on the quality of the welded joint [28] is the shielding gas. In general, the shielding gas used in HLAW contains a high percentage of inert gas such as argon (Ar) and helium (He). During hybrid laser arc welding with CO_2 laser, absorption of the laser energy by the laser induced plasma and reduction of the laser intensity that reaching the weld pool is often occurred, due to longer wavelength [40]. The use of high ionization potential shielding gas like helium reduces the effect of plasma absorption, therefore during hybrid laser arc welding with CO_2 laser, a mixture of argon, helium and CO_2 is used [35, 38, 40]. The use of helium ensures deeper penetration, the argon improves the arc stability, while a small percentage of oxygen less than 5% reduces the spatter formation and improves metal transfer during the welding process [42, 43]. The mode of metal transfer is an influential parameter for stable and repeatable welding process, for hybrid laser arc welding pulsed/spray-arc is recommended in relation to short/globular-arc [34, 43].

The angle of electrode is a parameter that affects the penetration of the weld provided by HLAW, this angle is related with the shielding gas flow and thus directly affecting the laser energy absorption [44]. The angle of electrode is typically set around 45^o – 65^o from the welding material surface, which reduces the arc length, and the laser beam is focused on the welding pool [36]. Generally, the laser beam is directed normal to the welding material surface to obtain better penetration. However, during the welding of highly reflective materials the laser beam is tilted at an angle in order to avoid any damages of the laser head due to the reflected beam, that must be different from the electrode's angle [45].

The main advantage of hybrid laser arc welding is the high welding speed and it's strictly related to the weld penetration. However, weld width and weld penetration are inversely affected by the welding speed [7, 9, 46]. The weld penetration increases when the welding speed decreases as a result of the higher heat input per unit length of weld [46]. The gap filling capability is improved at lower welding speeds, at constant filler wire feed rate [47]. The welding speed to filler wire feeding ration is an important factor for the stability of the keyhole and thus for the stability of the process itself [13, 17]. On the other hand, a too high welding speed leads to a fast heating and cooling cycle in the workpiece, which may result in metallurgical

defects in weld fusion zone. Too low welding speed may create a larger weld pool with deep penetration until the limit of burn through the welding material [48,49].

In HLAW, the laser power is the main heat source for the welding efficiency improvement, which produces the keyhole and ensures the deep penetration [21, 50]. Therefore, the ratio of the power of the two heat sources should be considered and obtained by dividing the laser power with the arc power [48, 49]. The geometry and metallurgical properties of the weld strictly depend on the balance between the influences of the laser source and arc source [50]. In HLAW increasing of the power ratio leads to a narrow weld width, reducing the tendency of grain growth and modifies the microstructure of fusion zone [16, 45, 51, 52]. In conditions of constant filler wire feed rate and laser power, a higher power arc causes an increase of the width of the bead until it reaches a maximum value [53]. This effect mainly is caused by the arc power, by increasing the voltage at constant filler wire feed speed, the arc length and its diameter grow up and consequently the area of molten pool grows up [16, 51, 53]. Under appropriate welding parameters, hybrid laser arc welding with high power ratio can ensure higher welding speed with better shape and microstructure of the weld, and thus directly affecting its mechanical properties [33, 54].

3. HLAW performance and characteristics

Welding performance of HLAW is measured in terms of weld penetration, increase of welding speed, and gap bridging ability while reducing the operative costs. The weld quality achieved by HLAW can be assessed in terms of improving the microstructure of the weld and its mechanical properties by reduction of the welding defects [57].

The laser beam welding provides high welding speed and high weld quality, but on the other hand requires precise preparation of the welding groove and set-up of the welded elements, which is not the case for HLAW [16]. For comparison, the HLAW process is 50% faster than the laser beam welding [49].

For hybrid welding of thin sheets and elements with different thickness, a combination Nd:YAG laser and MIG/MAG welding with thinner wire is used. On the other hand, for welding of thicker elements, a combination of gas CO2 laser with continuous wave with MIG electric arc is used [16, 58]. The HLAW enables welding of thin sheets at high welding speed in the range of 4m/min – 14m/min [59, 60]. The researchers Kutsuna and Chen compared the hybrid CO2 laser MIG/MAG welding of a low carbon steel with laser welding and found 30% faster welding speed during the hybrid welding. Additionally, the Nielsen's results showed that the welding speed can be increased in the range of 30%-100% during hybrid CO2 laser MIG/MAG welding of C/Mn steel compared to laser welding using cold filler wire. According to Frostevarg and Kaplan, the speed can be further increased up to 200% when a joint gap of 0.6mm is constant between the welding elements [63]. The results obtained through numerical simulation, showed that the HLAW enables double welding speed compared to laser welding for identical laser beam parameters [64]. Moreover, the hybrid laser arc welding produced weld joints with higher strength and ductility than classic laser beam welding, due to the use of filler wire [65].

Based on the previous research, cross-sections of the weld joint provided by hybrid welding was divided in two zones: the upper-wide zone or laser-arc region and lower-narrow zone or laser region [66]. In both zones, the difference is terms of microstructure and distribution of alloying elements, due to the temperature difference and crystallization process [53, 67, 68, 69].

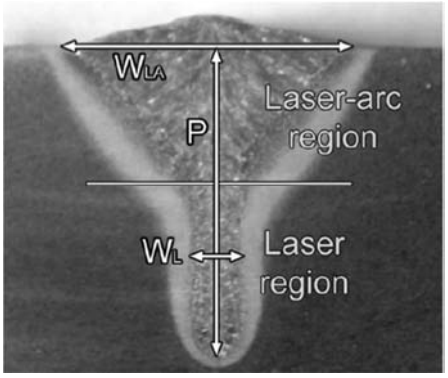

Figure 3. *Geometric characteristics of the HLAW weld cross-sections [4]*

Slika 3. *Geometrijske karakteristike poprečnog preseka HLAW zavarenog spoja [4]*

Except for thin sheets, the HLAW is used for thick sheets welding and usually is applied for thickness that can be welded in a single pass [56]. The steel plates with thickness up to 15mm are successfully welded in a single pass with a welding speed of 1 m/min by using a hybrid 20 kW laser MAG welding system [71]. Also, the constructive steel plates with thickness of 30mm can be welded, in dual passes using Hybrid welding with Double Rapid Arc – HyDRA, where two MAG torches are placed in two different sides of the plates [26]. In addition, steel plates with higher thickness can be welded by hybrid laser arc welding with multiple weld passes and optimum joint gap between the welding elements [72, 73]. The HLAW is capable to bridge a joint gap up to few millimeters depending on the laser power, welding speed, filler wire feed rate as well as the material thickness [74, 76]. However, by increasing the thickness of the welding elements, the possibility of pores and hot cracks in the weld increases as well [78, 79]. The second type of weld imperfections are more critical due to their sharpness [80, 81].

4. Industrial application of HLAW

Today, the hybrid laser arc welding represents an attractive alternative welding process for the different industries, due to several process advantages, such as: better weld quality and higher productivity compared to laser welding or arc welding [17, 82]. The initial costs for procurement of the entire hybrid process equipment can be compensated by providing higher welding speed and deeper penetration in order to reduce the cost per unit length of weld [41, 46]. With HLAW a wide range of materials, from ferrous metals like structural steels, stainless steels to non-ferrous metals like aluminum (Al), magnesium (Mg), Nickel (Ni) and their alloys can be welded [7, 16, 22, 31, 33, 83]. Moreover, HLAW allows the welding of thin sheet metals as well as thick metal plates in one or more weld passes, however compared to conventional welding processes the number of passes are less which results in reduction of weld distortion [30, 73, 79, 94].

5. Conclusion

The synergy effect of laser beam and electric arc offers several advantages over other individual technological processes, such as: increased productivity, deeper penetration, higher welding speed, better gap bridging ability, better process stability, less heat input to the welding material, etc. Nevertheless, the combination of two heat sources

The main application of HLAW process is found in automotive and shipbuilding industries, where producing light or heavy vehicles and ships a large number of metal components should be welded [85, 86].

In the automotive industries, companies like Audi AG and Volkswagen have already implemented hybrid laser arc welding in their production lines [87]. Total 48 hybrid fillet and butt welds are made in each of the Volkswagen Phaeton main frame, while the roof frame and its different parts of Audi A8 vehicle are welded by hybrid laser arc welding [88]. The HLAW process is also installed in Daimler AG and has resulted in increased productivity by increasing welding speed and wire efficiency, while maintaining good penetration and improved metallurgical characteristics of the welded joint [59].

The German shipyard company, Mayer-Werft GmbH in its own production line has implemented HLAW process for welding of steel panels and stiffeners that are installed in ships. By using a combination of 12 kW CO2 laser with a 450A GMAW, 12mm thick fillet joints with 12m long weld seams are performed successfully with reduced deformation and thus eliminates the reworking required for flattening of the welded parts. Pieces of tensile, hardness, impact, bending, and fatigue tests were performed from these joints and satisfactory results were obtained [89]. The Italian shipyard company, Fincantieri SpA by using hybrid laser arc welding system with combination of Nd:YAG laser and MAG welding technique, enabled them to overcome the problems with weld distortion and effective bridging of the joint gap [90]. For the shipbuilding industry the HLAW process with fiber laser has been developed and it integrates several software solutions for process control and weld quality monitor [91, 92].

The HLAW is used in power industry to weld tight wall panels and ribbed pipes of boilers, the company Energoinstal SA has applied hybrid laser arc welding due to its advantages, such as process stability, higher joint gap tolerance, higher efficiency and deep penetration [94].

5. Zaključak

Sinergijski efekat laserskog snopa i električnog luka dovodi do niza prednosti u odnosu na pojedinačne tehnološke procese zavarivanja, kao što su: povećana produktivnost i penetracija, veće brzina zavarivanja,bolja ispuna žlebova, bolja stabilnost procesa, manji unos toplote u radni materijal itd. Međutim, spajanje dva izvora toplote u

in a single welding process is challenging due to the increased number of welding parameters that should be synchronized, thus increasing the physical complexity of the process. The values of the parameters that are optimal for each process separately, are not suitable for hybrid laser arc welding, therefore the desired benefits can be obtained by appropriate combination of both heat sources and optimization of the welding parameters. In HLAW the laser power is the primary source of heat on which overall process and the welding penetration depth efficiency depends, while the power of the electric arc and its distance to the laser beam directly affects the process stability, droplet transfer mood and weld bead geometry. The ratio between the welding speed and filler wire feeding is another parameter that affects the entire process stability as well as on the weld shape. Similarly to other welding processes, in HLAW the shielding gas influences the arc characteristics, formation of weld shape, and mode of metal transfer. With hybrid laser arc a few millimeters joint gap welding successfully can be welded, but this distance also depends on the thickness of the materials, layout and ratio between both heat sources, welding speed and wire feed rate.

Despite the fact that the hybrid laser arc welding has been accepted by large number of industries and a good number of research have been published related to the advantages of its implementation, its percentage presence in the production lines is far from satisfactory, partly due to higher initial cost, partly due to the large number of process parameters and their mutual influences that have not been sufficiently explored, leading to entire hybrid arc welding process to be insufficiently developed.

For a better understanding of the HLAW process, besides the previous research and implementations, additional simulations and theoretical modeling are necessary to be performed as well as experimental research regarding efficiency and effectiveness of the entire process for welding of structural steel using different types of wires, solid and flux-cored welding wires. Moreover, due to the lack of information about the effects of different shielding gases and different welding wires as well as the influence of the welding groove shape on the quality and mechanical properties of the welded joints, additional experimental research should be performed.

jedan proces zavarivanja predstavlja izazov zbog povećanog broja parametara zavarivanja koje treba sinhronizovati, čime se povećava fizička složenost procesa. Vrednosti parametara koji su optimalni za svaki proces pojedinačno, nisu pogodni za hibridno zavarivanje sa laserskim snopom i električnim lukom, zbog toga jedini način za dobar kvalitet se može postići sa odgovarajućom kombinacijom oba izvora toplote i optimizacijom parametara zavarivanja. Kod hibridnog zavarivanja sa laserskim snopom i električnim lukom, snaga lasera je osnovni izvor toplote od kog zavisi efikasnost celog procesa i veličina prodiranja zavara, dok snaga i položaj elekričnog luka direktno utiču na stabilnost procesa, način prenošenja rastopljenog materijala i oblika zavara u gornjoj zoni. Na stabilnost celog procesa, kao i na oblik zavara utiče odnos između brzine zavarivanja i brzine prenošenja dodatnog materijala. Kao i kod drugih procesa zavarivanja, kod hibridnog zavarivanja zaštini gas utiče na karakteristike luka, formiranje oblika zavara i način prenošenja dodatnog materijala. Hibridno zavarivanje sa laserskim snopom i električnim lukom omogućavaju uspešno punjenje zazora do nekoliko milimetara, ali ovo rastojanje takođe zavisi od debeljine materijala, odnosa između dva izvora toplote i njihovog rasporeda, kao i od brzine zavarivanja i brzine prenosa dodatnog materijala.

Uprkos činjenici da je hibridno zavarivanje sa laserskim snopom i električnim lukom uveliko prihvaćeno od industrije i da je sprovođen neznatan broj istraživanja u vezi prednosti njegove implementacije, njegov udeo u proizvodnim linija daleko je od zadovoljavajućeg, delimično zbog početnih visokih troškova implementacije, delom i zbog velikog broja parametara samog procesa i njihovih međusobnih uticaja koji nisu dovoljno istraženi, što dovodi do toga da je ceo proces hibridnog zavarivanja sa laserskim snopom i električnim lukom nedovoljno razvijen.

Za bolje razumevanje procesa, pored dosadašnjih istraživanja i implementacije, neophodne su dodatne simulacije i teorijsko modeliranje, kako i sprovođenje dodatnih eksperimentalnih istraživanja i efektivnosti procesa pri zavarivanju konstrukcionog čelika korišćenjem različitih vrsta dodatnih materijala, pune i punjene žice. Dodatno, zbog nedostatka informacija trebalo bi ispitati kako debeljina radnog materijala, različiti zaštitni gasovi i žice za zavarianje, kao i uticaj oblika žljeba za zavarivanje utiču na kvalitet i mehanička svojstva zavarenih spojeva.

At the end, economic analysis for hybrid laser arc welding of structural steel should be performed in order to check the economic viability to achieve higher quality at lower costs compared to the individual welding processes.

Na kraju, treba sproveti ekonomsku analizu zavarivanja konstrukcionih čelika hibridnim zavarivanjem sa laserskim snopom i električnim lukom, kako bi se proverila ekonomska opravdanost za postizanje većeg kvaliteta uz niže troškove u odnosu na pojedinačne procese zavarivanja.

References / Literatura

[1] Agrawal B.P. and Kumar R., *Int. J. Eng. Res. Technol.*, 5, (2016), 319–327.

[2] Pal K. and Pal S.K., *Eng. Perform.*, 20, (2011), 918–931.

[3] Petring D., In: S Katayama (ed.). Cambridge: Woodhead Publ., 2013, 478–504.

[4] Wallerstein D., et al., *Mech Eng. Sci. 0(0),* (2020), 3-14.

[5] Nguyen T.C, et al., *Weld J.*, 86, (2007), 360–372.

[6] Piekarska W., et al., *Archives of metallurgy and mat.,* 56, (2011), 409-421.

[7] Bunaziv I., et al., *The Int. J of Adv. Man. Tec.,* 107, (2020), 2649-2669.

[8] Moore P.L, et al., *Sci. Technol. Weld Join*, 9, (2004), 314–322.

[9] Rao Z.H, et al., *Sci. Technol. Weld Join,* 16, (2011) 300–305.

[10] Le Guen E., et al., *Opt. Laser Technol,* 43, (2011) 1155–1166.

[11] Steen W. M, et al., *The 4th Int. Con. on Advances in Welding Processes* 1, (1978), 257-265.

[12] Ready J.F, Ind. Applications of Lasers. 2nd ed. London: Academic press, 1997.

[13] Seyffarth P., Krivtsun I.V., London: Taylor & Francis, 2002.

[14] Finke B.R., et al., *DVS-Ber,* 135, (1991), 149–152.

[15] Dilthey U., Wieschemann A., *Rivista Italiana della Saldatura,* 52 (6), (1999), 749-759.

[16] Runchev D., Tehniki na spojuvanje. Univerzitet “Sv. Kiril i Metodij”, Skopje, 2014.

[17] Petring D., Fuhrmann C., *The 1st Pacific Int. Con. on App. of Lasers and Optics*, (2004),.7-10.

[18] Tenner F., et al., *Phys. Procedia*, 56, (2014), 1268–1276.

[19] Roepke C., et al., *Weld J.*, 89, (2010) 140s–150s.

[20] Liu S., et al., *Opt. Laser Technol*, 44, (2012), 1019–1025.

[21] Bagger C., et al., *The 9th Nordic Laser Mat. Pro. Con.,* (2003), 113–124.

[22] Liu W., et al., *J. Mater. Process Technol.*, 214, (2014), 2823–2833.

[23] Gu X., et al., *Optics & Laser Tec.*, 48, (2013), 246–253.

[24] Blecher J.J., et al., *Weld J.,* 94, (2015), 73–82

[25] Pan Q., et al., *Weld World* 60, 4, (2016), 653–664.

[26] Webster S., et al. *Ironmak Steelmak,* 35(7), (2008), 496– 504.

[27] Bunaziv I., et al., *Opt. Lasers Eng.* 102 (supplement C), (2018a), 34–44.

[28] Kah P, et al., *J Eng. Man.,* 225, (2011), 1073–1082.

[29] Casalino G., et al., DAAAM int. sci. book 2010. Vienna: DAAAM Int., (2010), 413–430.

[30] Zhan X., et al., *Optics & Laser Tec.,* 85, (2016), 75–84.

[31] Thorny C., *Welding in the World,* 46(9), (2005), 88-98.

[32] Petring, D., et al., *Laser Mat. Pro. Conf. ICALEO*, (2007), 300-307.

[33] Eriksson I., et al.,. *Phys Proc*, 41, (2013), 119–127.

[34] Bagger, C. and Olsen, F.O., *J. Laser. Appl.* 17, (2005), 2–14.

[35] Ma N., et al., *J of Mat. Pro. Tec.,* 220, (2015), 36–45.

[36] Liu L., et al., *Transactions,* 47 (6), (2006), 1611-1614.

[37] Ribic B., et al., *Sci. Technol Weld Join*, 13, (2018), 683–693.

[38] Bunaziv I., et al., *J of Mat. Pro. Tec., 233,* (2016), 107–114.

[39] Huang R. S., et al., *J of Mat. Eng. and Perf.,* 17(6), (2008), 928– 935.

[40] Liu S., et al., *Optics & Laser Tec.*, 44, (2012), 1019–1025.

[41] Wahba M., et al., *Mater. Des.,* 97, (2016), 1–6.

[42] Sathiya P., et al., *Optics & Laser Tec.,* 45, (2013), 46–55.

[43] Campana G., et al., *J. of Mat. Pro. Tec.,* 191, (2007), 111–113.

[44] Wei H.L., et al., *Weld J.*, 94, (2015), 135–144.

[45] Liu T., et al., *Optics & Laser Tec.,* 80, (2016), 56–66.

[46] Bidi L., et al., *Optics & Laser Tec.,* 43, (2011), 537–545.

[47] El Rayes M., et al., *Weld J*, (2004), 147-153.

[48] Kong F., et al., *J. of Ma. Pro. Tec.,* 211, (2011), 1102–1111.

[49] Nilsson K., et al., *Proc. of 56th Annual Assembly of the Int. Ins. of Welding.* IIW Doc. IV-843-03, 2003, Bucharest, Romania.

[50] Turichin G., et al., *Procedia CIRP*, 74, (2018), 748–751.

[51] Thewlis G., *Mater. Sci. Technol.,* 20, (2004), 143–160.

[52] Frostevarg J., *J. Laser Appl.* 28:022407, 2016.

[53] Kah P., *Rev. Adv. Mater. Sci.*, 30, (2012) 112–132.

[54] Unt A., et al., *Phys Proc,* 78, (2015), 45–52.

[55] Leo P., et al., *Optics & Laser Tec.*, 73, (2015), 118–126.

[56] Acherjee B., *Optics & Laser Tec.*, 99 (1), (2018), 60–71.

[57] Mazar Atabaki M., et al., *Mater. Des.,* 67, (2015), 509–521.

[58] Wahba M., et al., *J. Mater. Pro. Tec.,* 221, (2015), 146–153.

[59] Staufer H., *Welding J.,* 86, (2007), 36–40.

[60] Jokar M., et al., *Iran J. Phys. Res.*, 14, (2014), 41–46.

[61] Kutsuna M., Chen L., *Int. Ins. of Welding,* IIW document, XII 1708-02, 2002.

[62] Nielsen S.E, et al., *Int. Ins. of Welding,* IIW doc. XII 1731-02, 2002.

[63] Frostevarg J. and Kaplan AFH., *Phys. Proc.*, 56, (2014), 663–672.

[64] Piekarska W., Kubiak M., *App. Math. Modelling,* (37), (2013), 2051–2062.

[65] Gao M., et al., *Sci. Technol. Weld Join*, (13), (2008), 106–113.

[66] Papaefthymiou S.A., *Int. J. Struct. Integrity,* 4, (2013), 91–107.

[67] Gao M., et al., *Appl. Surf. Sci.*, 254, (2008), 5715–5721.

[68] Campana G., et al., *J. Mat. Pro. Tec.*, 191, (2007), 111–113.

[69] Katayama S., et al., *Weld J.*, 21, (2007), 25–31.

[70] Shanping L., et al. *J. Mat. Sci.,* 40, (2005), 2481–2485.

[71] Sokolov M., et al., *Mater. Des.,* 32, (2011), 5127–5131.

[72] Üstündağ Ö., et al., *J. Mat. Pro. Tec.*, 275: 116358, 2020.

[73] Bunaziv I., et al., *Phys. Procedia* 78 (supplement C), (2015), 74–83.

[74] Gebhardt MO., et al., *Sci. Tec. Weld Join*, 19, (2014), 209–213.

[75] Shi S., *Int. Forum on Welding Tec. in Energy Eng*. Shanghai, China, 2005.

[76] Qi Y., Chen G., *J. Mat. Pro. Tec.,* 260, (2018), 97–103.

[77] Reutzel E.W., et al., *J. Ship. Prod.*, 24(2), (2008), 72–81.

[78] Chen Y., et al., *Mat. Sci. Eng. A.*, 582, (2013), 284–293.

[79] Bunaziv I., et al., *J. Mat. Pro. Tec.* 256, (2018d), 216–228.

[80] Bunaziv I., et al. *Int. J. Adv. Man. Tec.*, 102(5), (2019), 2601–2613.

[81] Mu Z., et al., *Int. J. Heat Mass. Transf.,* 132, (2019), 861–870.

[82] Chung B., et al., *Mater. Sci. Eng. A.*, 272, (1999), 357–362.

[83] Grunenwald S., et al., *Phys. Procedia*, 5, (2010), 77–87.

[84] Cai X., et al., *Int. J. Adv. Man. Tec.*, 91, (2017), 3449–3456.

[85] Reutzel E.W., et al., *Welding J,* 85 (6), (2006), 66-71.

[86] Zhen S., et al., *Opt. Laser Tec.*., 59, (2014), 11–18.

[87] Staufer H.,. *The 3rd Int. WLT-Con. on Lasers in Man. Conf.*, Munich, Germany, 2015, 203–208.

[88] Lee M., et al., *The Laser Mat. Pro. Con. ICALEO*, Miami, USA, 2005, 134-142.

[89] Roland F., et al., *The IIW Int. Con. in Connection with Annual Assembly*, Copenhagen, Denmark, 2002, 103–115.

[90] Gerritsen C.H.J, et al., *The 10th Nordic Laser Mat. Pro. Con.,* Lulea, Sweden, 2005, 395-406.

[91] Jasnau U. and Sumpf A., *The Nordic Welding Con.,* Tampere, Finland, 2006.

[92] Orozco N.J., *The Laser Mat. Process Con. ICALEO*, Jacksonville, USA, 2003, 31–40.

[93] Webster S.E., et al., *Hyblas: economical and safe laser hybrid welding of structural steel.* Luxembourg City, Luxembourg, 2009.

[94] Adamiec J., et al., *Welding Int.,* 24 (11), (2010), 853-860.

[95]www.fronius.com/en/welding-technology /products/robotic-welding/migmag-high-performance/laserhybrid/laserhybrid [Accessed on 30th March 2021].

[96] Wallerstei D., et al., *J. Mec. Eng. Sci,* 0(0), (2020), 1-14.

Podsećamo vas da je sada vreme da obnovite vaše članstvo u DUZS i pretplatu za naš časopis.

Li hong[1,a], Liu Xusheng[1,b], Wang bing[2,c], Li Zhuoxin[1,d]

Effect of post-weld tempering treatment on performance of DP600 spot welded joint

Uticaj obrade otpuštanjem nakon zavarivanja na osobine tačkasto zavarenog spoja dvofaznog čelika DP600

Stručni rad / Professional paper

Rad je u izvornom obliku objavljen u okviru 72. IIW godišnje Skupštine i međunarodne konferencije održane u Bratislavi-Slovačka 07-12. Jula 2019

Rad primljen / Paper received:
Oktobar 2020.

Prevod izvornog rada na srpski jezik: Z. Odanović

Adresa autora / Author's address:

[1]Beijing University of Technology, College of Materials Science and Engineering, Beijing, China

[2]Hefei General Machinery Research Institute, College of Materials Science and Engineering, Hefei, China

[a]lih_bjut@163.com,

[b]lxs_bjut@163.com,

[c]1481202485@qq.com,

[d]13910321588@139.com

Keywords: DP600, resistance spot welding, tempering treatment, fatigue strength

Abstract

In order to meet the increasing requirements of the automotive industry for material strength grades and performance, the application of advanced high-strength steel automotive panels, represented by dual-phase steel, in lightweight vehicle bodies is increasing. Resistance spot welding is the main joining process for vehicle body manufacturing. How to improve the tensile strength and fatigue performance of dual-phase steel resistance spot welding joints is of great significance to the welding structure of the body. In this paper, resistance spot welding of cold rolled DP600 dual phase steel in the welding current range of 9000A-12000A was carried out. The effects of post-weld tempering treatment on microstructure, microhardness, shearing and fatigue of joints were compared. The results show that the microstructure transformation occurs in the weld nugget area after post-weld tempering, and the tempered martensite appears to reduce the microhardness of the weld nugget area; the nugget diameters, tensile-shear strength and failure energy are all higher than those without tempering treatment; tempering improves the fatigue strength of the spot joints, and regardless of whether the welded joints are tempered, cracks are all generated near the heat affected zone of the joint after fatigue test.

Ključne reči: čelik DP600, elektrootporno tačkasto zavarivanje, obrada otpuštanjem, zamorna čvrstoća

Rezime

U cilju postizanja povećanih zahteva automobilske industrije za čvrstoćom i osobinama materijala korišćenih u proizvodnji, porasla je primena naprednih čelika visoke čvrstoće za izradu panela za karoserije vozila, posebno od dvofaznih čelika. Tačkasto elektrootporno zavarivanje je glavni proces spajanja pri proizvodnji karoserija vozila. Način unapređenja zatezne čvstoće i osobina otpornosti na zamor elektrootporno tačkasto zavarenih spojeva dvofaznih čelika je od velikog značaja za zavarene konstrukcije karoserija. U ovom radu, ispitivano je elktrootporno tačkasto zavarivanje hladno valjanog dvofaznog čelika, pri struji zavarivanja u opsegu od 9000A-12000A. Poređeni su efekti otpuštanja nakon zavarivanja na mikrostrukturu, mikrotvrdoću, smicanje i zamor spojeva. Rezultati pokazuju da se mikrosturkturne transformacije dešavaju u oblasti sočivastog šava otpuštanjem nakon zavarivanja i da otpušteni martenzit koji se javlja, snižava mikrotvrdoću sočivastog šava, a prečnik šava, zatezno-smicajna čvrstoća i enrgija loma su više u odnosu na one bez obrade otpuštanjem. Otpuštanje poboljšava zamornu čvrstoću tačkastog spoja i bez obzira da li je otpušten, prsline se stvaraju uz zonu uticaja toplote spoja nakon ispitivanja zamaranjem.

1. Introduction

In order to meet the needs of the automotive industry for the light weight and safety performance of the car body, the development of lightweight high-strength advanced highstrength steel has become the key to lightweight technology [1]. As a typical representative of the first generation of advanced high-strength steel, Dual Phase steel has the advantages of high strength, good elongation, formability, and strong absorption of collision energy. Now it has become the most extensive high-strength steel material used in the body weight reduction trend. It is mainly used in automotive parts requiring high strength, strong impact absorption resistance and good forming performance, such as hood, frame and wheel. With the advancement of steel properties and forming technology, Dual Phase steel is also used in parts such as interior and exterior panels of automobiles [2].

At present, in the manufacture of advanced high-strength steel sheet structures for automobile bodies, the spot welding process is relatively mature. Many studies on advanced highstrength steel resistance spot welding mainly focuses on the weldability of various steels, the influence of welding specification parameters on the microstructure of spot joints, the optimization of welding procedures and processes, etc., aiming to improving the quality of joints from the perspective of adjustment of welding process parameters. 590 MPa, 600 MPa, 780 MPa dual-phase steels have been confirmed to be welded by resistance spot welding, and A. Chaboket al. [3] found that double-pulse spot welding can also achieve high-strength connection of 1 000 MPa grade dual-phase steel; Tai-I Hsuet al.[4] compared the joint performance of the DP780 resistance spot welding and the friction stir spot welding. It was found that a larger spot joint area and a higher joint strength can be achieved by resistance spot welding; Besides the same material of dual-phase steel, Jian bin Chen]et al.[5] also studied the resistance spot welding of DP600 and 5052 aluminum alloy; S. H. Mousavi Anijdan et al. [6] studied the spot welding of DP600 with stainless steel. Taguchi method was used to design the experiments and Minitab software was used to analyze the effect of parameters and obtain an optimum condition. For the influence of parameters on spot welding of dual-phase, Mohsen et al. [7] analyzed the effects of welding current, welding time, electrode pressure and electrode size on the performance of DP600 joints; Wang et al.[8] used finite element simulation to analyze the

1. Uvod

U cilju postizanja zahteva automobilske industrije za smanjenjem težine i sigurnosti karoserija vozila, razvoj lakih, naprednih čelika visoke čvrstoće je postao glavni imperativ tehnologija smanjenja težine [1]. Kao izraziti predstavnik prve generacije naprednih čelika visoke čvrstoće, dvofazni čelik (DP) imao je prednosti visoke čvrstoće, dobrog izduženja, plastičnosti i visoke absorbcije energija sudara. On je postao najčešće korišćeni čelični materijal visoke čvrstoće u cilju smanjenja težine. On se uglavnom koristi za delove vozila koji zahtevaju visoku čvrstoću, visoku otpornost na snažne udare, kao i dobre osobine za oblikovanje, za delova kao što su hauba, šasija i točkovi. Sa prednostima koje karakterišu čelike i razvijene tehnologije oblikovanja dvofaznog čelika (DP), omugućavaju njegovu primenu za delove kao što su unutrašnji i spoljašnji paneli automobila [2].

U proizvodnji naprednih struktura za karoserije automobila od čeličnih limova visoke čvrstoće, proces tačkastog zavarivanja je relativno sazreo. Mnoge studije o otpornom tačkastom zavarivanju naprednih čelika visoke čvrstoće, uglavnom su se usresredile na zavarljivost različitih vrsta čelika, uticaj parametara zavarivanja na mikrostrukturu tačkastog spoja, optimizaciju procedura i procesa zavarivanja i slično, imajući za cilj poboljšanje kvaliteta spoja iz ugla podešavanja parametara procesa zavarivanja. Za dvofazne čelike klase 590 MPa, 600 MPa i 780 MPa, potvrđeno je da se uspešno zavaruju otpornim tačkastim zavarivanjem, a A. Chaboket i dr. [3] su našli da duplo pulsirajuće tačkasto zavarivanje može takođe da postigne spoj visoke čvrstiće i kod dvofaznih čelika klase 1000 MPa. Tai-I Hsuet i dr. [4] su poredili osobine spoja čelika DP780 koji su tačkasto zavareni i zavarenih postupkom zavarivanja trenjem sa mešanjem. Pokazano je da se može postići veća oblast tačkastog spoja i veća čvrstoća tačkastim otpornim zavarivanjem. Pored ispitivanja spajanja istih materijala – dvofaznih čelika, Jian bin Chen]et i dr.[5] su ispitivali tačkasto otporno zavarivanje dvofaznog čelika DP600 i aluminijumske legure 5052. S. H. Mousavi Anijdan i dr. [6] su ispitivali tačkasto zavarivanje čelika DP600 sa nerđajućim čelikom. Taguchi metod je korišćen za kreiranje eksperimenata, a Minitab softver primenjen za analizu uticaja parametara na tačkasto zavarivanje dvofaznih čelika. Mohsen i dr. [7] analizirali su efekte jačine struje, vremena zavarivanja i pritiska i veličine elektroda na osobine spojeva čelika DP600. Wang i dr.[8] su koristili simulaciju metodom konačnih elemenata da bi

influence of pitting and size increase on the quality of DP590 dual-phase steel resistance spot welding. The results show that the two tip shapes will seriously affect the quality of the solder joints, so that the pull - shear strength is reduced. Li Hong et al. [9] studied the DP600 spot welding process and obtained the spot welding window and the best welding specifications. Zhang et al. [10] analyzed the failure modes of dual-phase steel resistance spot welded joints of different thicknesses, pointing out that tensile stress causes interface failure and shear stress causes pull failure.

However, advanced high-strength steel represented by dual-phase has a low carbon content and a high alloying element content [11]. During resistance spot welding, molten high-temperature austenite is rapidly cooled. (about 2000 oC/s) During the formation of nugget, the temperature curve will directly cross the martensite transformation critical region, and different contents and distribution of martensite will be produced in the nugget [12]. These martensites will make the nuclear hardness becomes higher and the brittleness increases. On the other hand, the cooling phase transformation produces defects such as pores, cracks and uneven internal stress distribution [13], which not only reduces the static load strength of the joint, but also shortens the low cycle fatigue life [14].

How to improve the problems mentioned above, in addition to adjust the welding process specifications, postweld treatment is a relatively good method. Wei shidong of Harbin Institute of Technology [15] found that the strength and plasticity of the dual-phase steel plate were significantly reduced after welding. The post-weld tempering treatment can eliminate the internal stress and transform the structure, thus improving the plasticity. M.S. Zhao et al. [16] found that proper post-weld heat treatment can improve the ductility and maximum bearing capacity of the workpiece. If the specimen is overheated, although the plasticity is likely to increase, the bearing capacity will be seriously degraded. Researches prove that the multi-pulse tempering process can fully temper the high stress area of the spot joint, and obtain the ductile fracture morphology. The mechanical properties, especially the fatigue performance, can be significantly improved.

Based on this research, this paper studies the effect of post-weld pulse tempering on the performance of cold rolled dual-phase steel DP600 resistance spot welded joints. Microstructure observation, hardness test, shear test and fatigue

analizirali uticaj pitinga i povećanja dimenzija na kvalitet tačkastog zavarivanja dvofaznog čelika DP590. Rezultati su pokazali da dva različita oblika vrha elektroda značajno utiču na kvalitet spoja, pa je zatezno smicajna čvrstoća smanjena. Li Hong i dr. [9] su ispitivali proces tačkastog zavarivanja čelika DP600 i dobili su najoptimalnije parametre zavarivanja. Zhang i dr. [10] analizirali su modele loma elektrootporno tačkasto zavarenih spojeva dvofaznih čelika različitih debljina, ističući da zatezni naponi uzrokuju medjupovršinski lom i da smicajni naponi prouzrokuju zatezne lomove.

Napredni čelici visoke čvrstoće predstavljeni dvofaznim čelicima imaju nizak sadržaj ugljenika i visok sadržaj legirajućih elemenata [11]. Za vreme elektrootpornog tačkastog zavarivanja, tečan visoko temperaturni austenit se brzo hladi brzinom od oko 2000 oC/s. Za vreme formiranja sočivastog šava, temperaturna kriva direktno prolazi kroz kritičnu oblast martenzitne transformacije i različita količina i raspodela martenzita nastaje u spoju [12]. Ovaj martenzit daje povišenje tvrdoće i krtosti. Sa druge strane, fazne transformacije pri hlađenju proizvode greške kao što su pore, prsline i neujednačenu raspodelu unutrašnjih napona [13], koji ne samo da smanjuju statičku čvrstoću spoja pri opterećenju, već skraćuju niskociklični zamorni vek [14].

Kako bi prevazišli gore pomenute probleme, a u cilju podešavanja karakteristika procesa zavarivanja, termička obrada nakon zavarivanja je relativno dobar metod. Wei Shidong iz Harbin Institute of Technology [15] je našao da se čvrstoća i plastičnost dvofaznih čeličnih limova značajno smanjuje nakon zavarivanja. Termički tretman otpuštanjem nakon zavarivanja, može da eliminiše unutrašnja naprezanja i da transformiše strukturu, čime se poboljšava plastičnost. M.S. Zhao i dr. [16] našli su da podesnom termičkom obradom nakon zavarivanja mogu da se poboljšaju plastičnost i naveća nosivost radnog komada. Ako se komad pregreje, iako izgleda da plastičnost raste, nosivost će biti značajno umanjena. Istraživači su potvrdili da proces otpuštanja u više ciklusa može da potpuno otpusti viske napone u oblasti tačkastog spoja i da se dobije duktilna morfologija loma. Mehaničke osobine, posebno osobine loma, mogu da se značajno unaprede.

Na osnovu ovih istrživanja, u radu su izučavani efekti procesa otpuštanja u više ciklusa na osobine spoja hladno valjanog dvofanog čelika DP600 koji je zavaren elektrootpornim tačkastim zavarivanjem. Ispitivanja mikrostrukture, tvrdoće, smicajne čvrstoće i zamora su izvršena na otpuštenim test

are carried out on the tempered joint. It was found that after post-weld tempering treatment, martensite transformation occurred in the microstructure of the joint, the hardness and brittleness phase decreased, and the shear strength and fatigue strength of the joint were improved.

2. Experiment

Cold-rolled DP600 dual-phase steel which is cut into 100mm×30mm×1mm is chosen for the study and the joint length of the spot welded joint is 30 mm. The nominal composition of this steel is shown in Tab. 1. From the metallographic structure (Fig. 1), we can see that the DP600 dual-phase steel is mainly composed of martensite and ferrite. The martensite is uniformly distributed on the ferrite matrix in island shape, showing obvious metal fiber flow lines. Soft ferrite and martensite are coexisted, and a small amount of light blue bainite exists on the martensite matrix at the ferrite interface.

spojevima. Utvrđeno je da nakon tretmana otpuštanjem posle zavarivanja, martenzitna transformacija se dešava u mikrostrukturi spoja i da se količina tvrdih i krtih faza smanjuje, čime se smicajna i zamorna čvrstoća spoja poboljšavaju.

2. Eksperiment

Hladno valjani dvofazni čelik DP600, isecan je u uzorke dimenzija 100mm×30mm×1mm, koji su izabarani za ispitivanja, a dužina spoja tačkasto zavarenog spoja je bila 30mm. Nominalni sastav ispitivanog čelika je prikazan u Tabeli 1. Iz metalografskih struktura prikazanih na slici 1, može se videti da je dvofazni čelik DP600 uglavnom sastavljen od martenzita i ferita. Martenzit je ravnomerno raspoređen u feritnoj osnovi u obliku ostrva, pokazujući očigledne linije trakavosti. Konstatovano je prisustvo ferita i martenzita, kao i mali udeli svetlo plavog beinita koji se javlja u martenzitnoj osnovi na feritnim međupovršinama.

Table 1. *Composition (mass fraction, %) and mechanical properties of DP600*

Tabela 1. *Hemijski sastav (u masenim udelima, %) i mehaničke osobine čelika DP600*

C	Mn	Si	Carbon equivalent Ugljenični ekvivalent/Ceq	Tensile strength Zatezna čvrstoća	Yield strength Granica tečenja
0.1	1.6	0.3	0.37	≥600MPa	≥350MPa

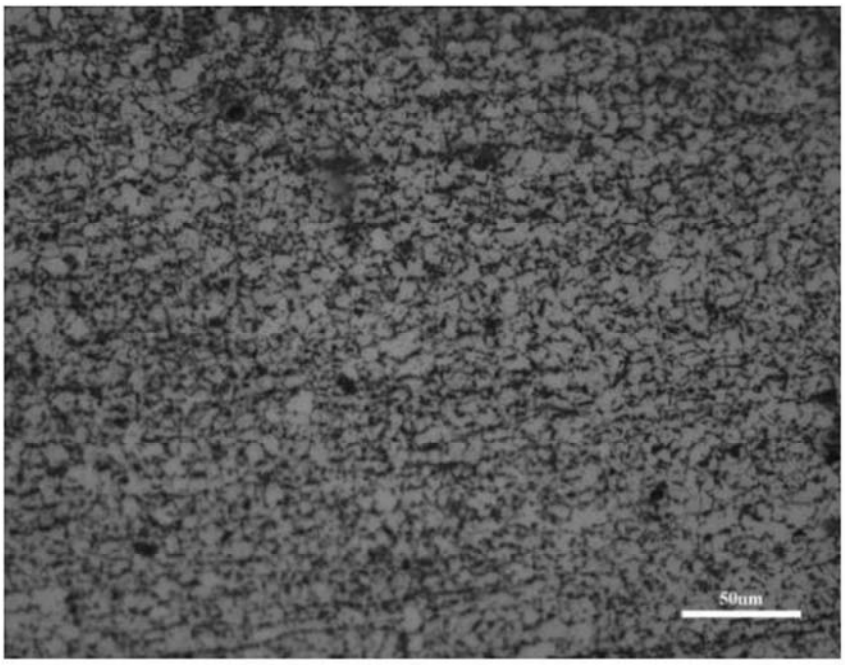

Figure 1. *The microstructure of DP600*

Slika 1. *Mikrostruktura čelika DP600*

Spot welding was performed using a ZPDN-90 medium frequency inverter resistance spot welding machine operating in the range of welding time is 200 ms, electrode force is 3 500 N and welding current is 9 000 A - 12 000 A. Then the workpieces were tempered with the time is 700 ms, temperature current is 6 000 A. The metallographic sample was prepared at the maximum cross-sectional area of the joint, then etched with 4% nitric acid alcohol solution, the microstructure of the structure was observed under OLYMPUS-BX51M metallographic microscope and OLYMPUS-SZ61 stereo microscope.

Mechanical properties of the spot welds are characterized using hardness profile, tensile test and fatigue test. Vickers hardness profile is measured along the diagonal direction of the spot welding sample, passing through the base material zone, the heat affected zone, the nugget zone and the heat affected zone with an indenting load of 200 g, a loading time of 10s and the distance of 0.2 mm. Fig. 2 is the testing track of micro-hardness.

Tačkasto zavarivanje izvršeno je srednje frekventnim invertorskim uredjajem ZPDN-90 za tačkasto zavarivanje, sa vremenom zavarivanja od 200 ms, silom pritiska elektroda od 3500 N i strujom zavarivanja od 9000 A - 12000 A. Zatim su uzorci otpuštani u vremenu od 700 ms, sa strujom od 6000A. Metalografski uzorci su pripremani iz maksimalne oblasti poprečnog preseka spoja. Nakon toga su nagrizani sa 4% rastvorom azotne kiseline u alkoholu i mikrostruktura je analizirana na metalografskom mikroskopu OLYMPUS-BX51M i stereo mikroskopu OLYMPUS-SZ61.

Mehaničke osobine tačkastih spojeva su određivane ispitivanjem tvrdoće, ispitivanjem zatezanjem i ispitivanjem zamorom. Linije na kojima je ispitivana Vikers trdoća su duž pravca dijagonale tačkasto zavrenog uzorka, prolazeći kroz osnovni metal, zonu uticaja toplote, metala šava i ponovo kroz zonu uticaja toplote. Merenje je vršeno sa opterećenjem od 200g, vremenom opterećenja od 10s i sa medjusobnim rastojanjem između otisaka od 0.2mm. Na slici 2 su prikazane linije ispitivanja mikro tvrdoće.

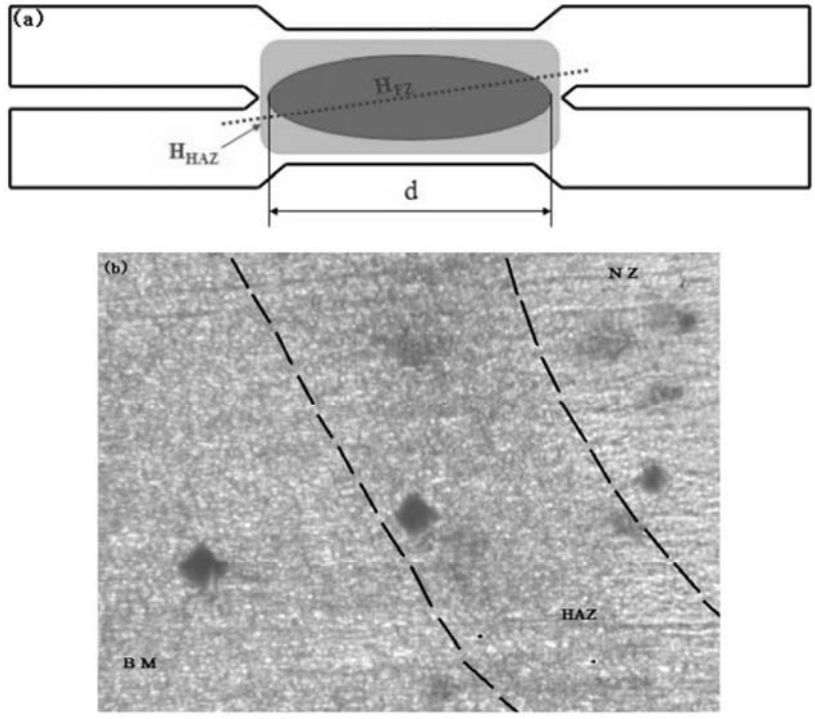

Figure 2. *The micro-hardness detection track: (a) sketch of hardness testing track; (b) hardness testing track under microscope*

Slika 2. *Linije ispitivanja mikro tvrdoće: a) šematski prikaz linija ispitivanja tvrdoće; b) linija ispitivanja tvrdoće na mikroskopu*

Tensile and fatigue tests were performed at room temperature with the MTS-810 Material Test System. Fig. 3 is the dimension of tensile-shear and fatigue specimens. Tensile tests were performed with a tensile strength speed of 5-6

Isptivanja zatezanjem i ispitivanja zamorom su vršena na sobnoj temperaturi sa sistemom za ispitivanje matrijala MTS-810. Na slici 3 su prikazane dimenzije uzoraka za ispitivanje smicanja zatezanjem i ispitivanja zamorom. Ispitivanje

mm/min and fatigue tests were performed with a frequency of 5–20Hz and a force ratio Rp (=Pmin/Pmax) = 0.1. In addition, the test was interrupted every 1×107 cycles. Peak load (measured as the peak point in the load–displacement curve) and failure energy (measured as the area under the load-displacement curve up to the peak load) were extracted from the load–displacement curve. The failure energy (energy absorption) was obtained by integrating the area under the load-displacement curve up to the peak load using the following equation(2-1)[17]:

$$\text{Failure energy} = \sum_{n=1}^{N} F(n)[X(n) - X(n-1)] \cdots\cdots (2-1)$$

where F is load, X is the displacement, n is the sampled data and N is the peak failure load. The data points for peak load and failure energy are the average of three samples.

The fatigue strength was obtained using the following equation(2-2) [18]:

$$\delta_{R(N)} = \frac{1}{m} \sum_{i=1}^{n} V_i \delta_i \cdots\cdots (2-2)$$

Where m is the total number of effective tests; n is the level of stress level; δ_i is the ith stress level; V_i is the number of tests at the ith stress level; $\delta_{R(N)}$ is the stress corresponding to 10^7 cycles.

zatezanjem vršeno je sa brzinom zatezanja od 5-6 mm/min, a ispitvanja zamorom su vršena sa frekvencijom od 5–20Hz i odnosom sila od Rp (=Pmin/Pmax)=0.1. Dodatno su ispitivanja prekidana svakih 1×10^7 ciklusa. Maksimalno opterećenje (mereno na vršnoj tački krive opterećenje – pomeranje) i energija loma (merena kao površina ispod krive opterećenje – pomeranje do vršnog opterećenja) koja je dobijena iz krive opterećenje – pomeranje. Energija loma (absorbovana energija) je dobijena integraljenjem površine ispod krive opterećenje – pomeranje do vršnog opterećenja primenom sledeće jednačine (2-1)[17]:

$$\text{Failure energy} = \sum_{n=1}^{N} F(n)[X(n) - X(n-1)] \cdots\cdots (2-1)$$

Gde je F – opterećenje, X je pomeranje, n je uzorkovan podatak i N je vršno opterćenje loma. Podaci za vršno opterćenje i energija loma su srednje vrednosti tri uzorka.

Čvrstoća loma je dobijena primenom sledeće jednačine (2-2) [18]:

$$\delta_{R(N)} = \frac{1}{m} \sum_{i=1}^{n} V_i \delta_i \cdots\cdots (2-2)$$

Gde je m ukupan broj testova, n je nivo napona, δ_i je i-ti nivo napona, V_i, je broj ispitivanja na i-tom nivou napona, $\delta_{R(N)}$ je napon koji odgovara 10^7 ciklusa.

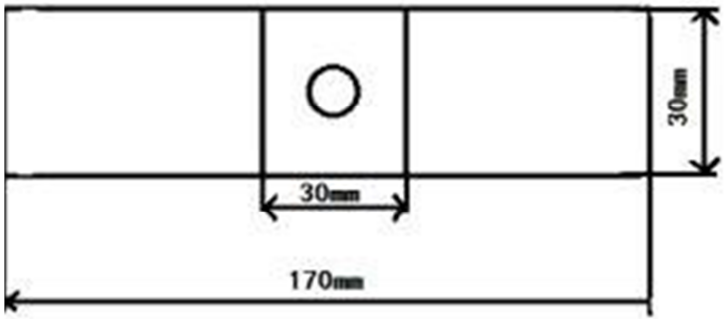

Figure 3. *Dimension of tensile-shear and fatigue specimens*

Slika 3. *Dimenzije uzoraka za ispitivanje smicanja zatezanjem i ispitivanje zamorom*

3. Results and discussion

3.1 Microstructure and microhardness

Fig. 4 shows the microstructure of the nugget area before and after tempering at the welding current: 12 000 A, welding time: 200 ms, welding load: 3 500 N. It can be seen that acicular martensite occurred in the tempered nugget area while there are mainly lath martensite in without tempered nugget zone.

3. Rezultati i diskusija

3.1 Microstruktura i mikrotvrdoća

Slika 4 pokazuje mikrostrukturu sočivastog šava pre i posle otpuštanja pri struji zavarivanja od 12000 A, vremenu zavarivanja od 200 ms, pritisku elktroda pri zavarivanju od 3500N. Može se videti da se igličasti martenzit javlja u oblasti otpuštenog sočivastog šava, dok je uglavnom lamelarni martenzit u neotpuštenoj zoni sočivastog šava.

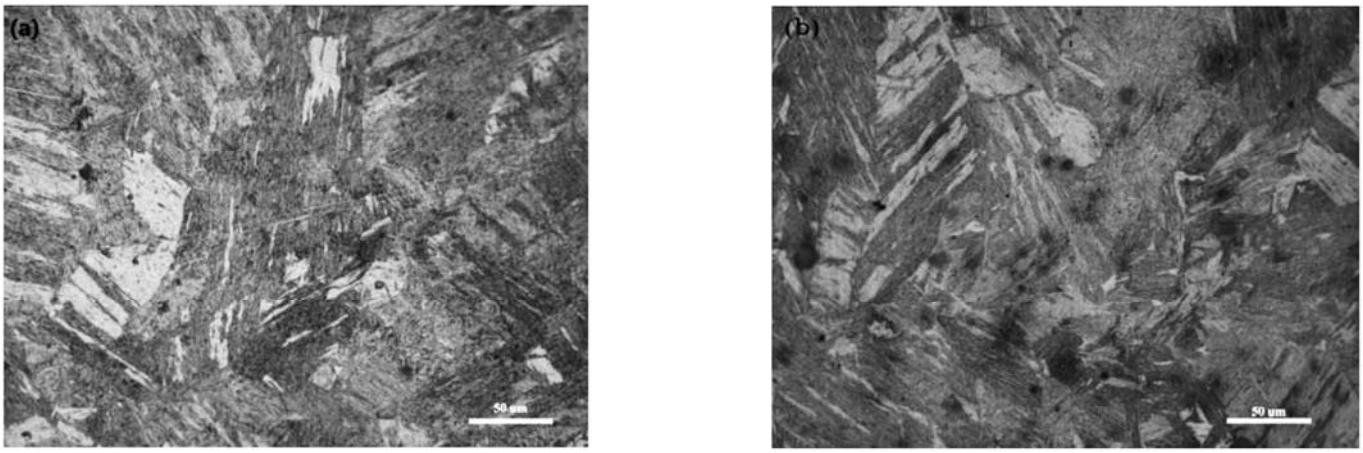

Figure 4. *Microstructure of nugget area before and after tempering: (a) without tempering; (b) tempered*

Slika 4. *Mikrostruktura sočivastog šava pre i posle otpuštanja: a) bez otpuštanja; b) nakon otpuštanja*

After the microhardness test, as shown in Fig. 5, it was found that the microhardness of the nugget after the tempering treatment decreased slightly, which indicate that the microstructure of the nugget region changed. The acicular martensite structure may be tempered martensite.

Nakon ispitivanja mikrotvrdoće, kao što je prikazano na slici 5, konstatovano je da je mikrotvrdoća sočivastog šava nakon tretmana otpuštanja neznatno smanjena, što ukazuje da je promenjena mikrostruktura oblasti sočivastog šava. Struktura igličastog martenzita, mogla bi da bude otpušteni martenzit.

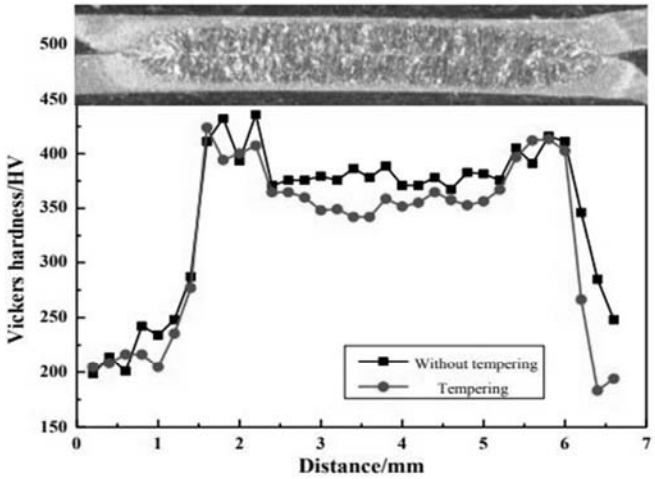

Figure 5. *Microhardness testing results, with and without temepering*

Slika 5. *Rezultati merenja mikrotvrdoća, pre i posle otpuštanja*

3.2 Mechanical Properties

Fig. 6 shows the measurement schematic diagram of nugget diameter. Fig. 7 is the welding current-nugget diameter relationship before and after tempering. It can be seen that before and after tempering, the welding current is 9000~12 000A, the diameter of the nugget increases with the increase of current and all the nugget diameters reach A grade, which is classified by Automotive industry and the United States RWMA on spot welding nugget, as shown in Tab. 2 (δ is the thickness of the base material) [19]. This phenomenon is related to the welding heat input.

3.2 Mehaničke osobine

Slika 6 šematski prikazuje merenje prečnika sočivastog šava. Slika 7 prikazuje odnos struje zavarivanja i prečnika sočivastog šava pre i posle otpuštanja. Može se videti pre i posle otpuštanja, pri struji zavarivanja 9000~12000A, da se prečnik sočivastog šava povećava sa povećanjem jačine struje i da svi prečnici sočivastog šava dostižu A kvalitet, koji je klasifikovan od strane Automobilske industrije i SAD RWMA za tačkasti sočivasti šav, kao što je prikazano u Tabeli 2. (δ je debljina osnovnog materijala) [19]. Ovaj fenomen je uslovljen unosom toplote zavarivanja.

When the welding current is small, the welding heat input will be reduced, the heating at the spot area will be insufficient, and the molten metal will be less, which directly leads to the smaller diameter of the weld nugget. As the welding current increases, the heat input increases, and the resistance heat is sufficient to melt more metal to form a high-quality nugget. The diameter of the nugget is inevitably increased. Xinge Zhang [20] and Xiaodong WAN [21] also pointed that if the welding current is too big, the expansion speed of the nugget diameter greatly exceeds the expansion speed of the plastic ring, splash will occur at the solder joint, and defects will be generated inside the nugget.

Kada je struja zavarivanja mala, unos tolote zavarivanja biće smanjen, i zagrevanje u oblasti tačkastog spoja će biti nedovoljno, što direktno dovodi do manjeg prečnika sočivastog šava. Sa povećanjem jačine struje zavarivanja, unos toplote se povećava, toplota nastala otporom je dovoljna da istopi više metala i stvori visoko kvalitetan sočivast šav. Prečnik sočivastog šava se neizbežno povećava. Xinge Zhang [20] i Xiaodong WAN [21] su takođe naglasili da ako je struja zavarivanja suviše visoka, brzina širenja prečnika sočivastog šava značajno prelazi brzinu širenja okolnog mekanog prstena i prskanje će se desiti u spoju koji očvršćava, čime će se formirati greška unutar sočivastog šava.

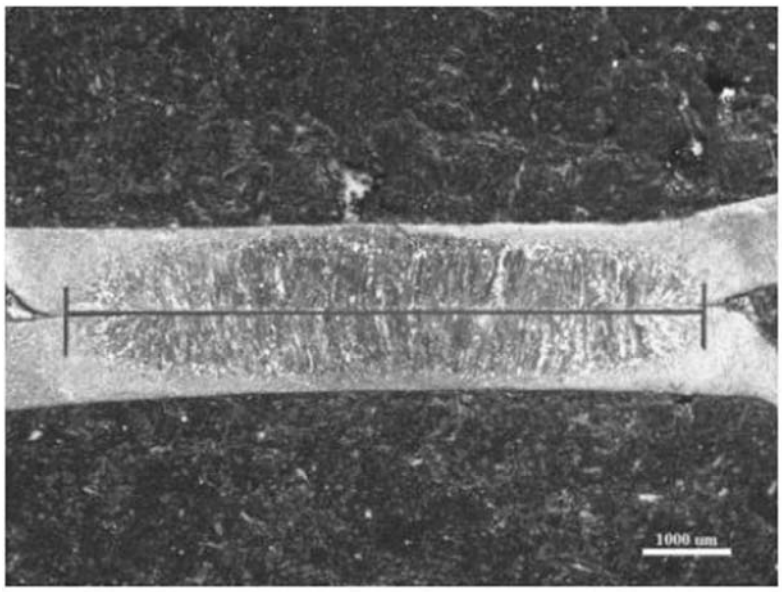

Figure 6. *Measurement schematic diagram of nugget diameter*

Slika 6. *Šematski dijagram merenja prečnika sočivastog šava*

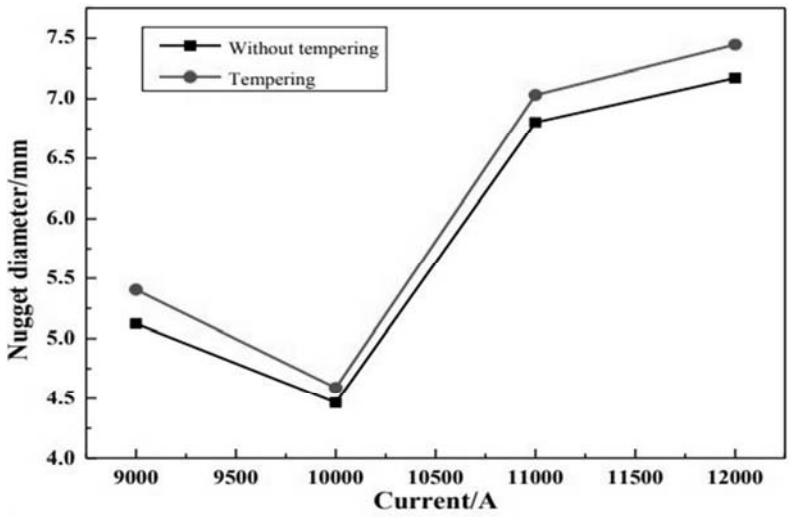

Figure 7. *Welding current-nugget diameter relationship before and after tempering*

Slika 7. *Zavisnost struje zavarivanja – prečnik sočivastog šava, pre i nakon otpuštanja*

Table 2. *The classification of nugget [19]*

Tabela 2. *Klasifikacija sočivastog šava [19]*

Grade/ Kvalitet	*A*	*B*	*C*
Diameter/ Prečnik	*5√δ*	*4√δ*	*3√δ*
Area/ Površina	*19.62δ*	*12.56δ*	*7.065δ*

Then we can find the spot weld nugget diameter without tempering is smaller than the tempered. Thus by post-weld tempering, we can obtain a larger spot joint. As studied by A.S. Baskoro et al. [22] that the diameter of the nugget has a great influence on the shear load of the spot welded joint. The larger the joint area, the larger the load it can bear. Fig. 8 shows the average tensile-shear force of the joint increases with the continuous increase of the welding current. Under the condition of tempering treatment, the maximum tensileshearing force is 14.0 1kN when the welding current is 12 000 A, while the maximum tensile-shearing force is 12.84 kN under the condition of without tempering treatment. Moreover, the average tensile shear force of the sample with tempered treatment is greater than that without tempering sample under the same parameters. Fig. 9 reveals the displacement distance of the tempered sample is much larger than that without tempering. It can be seen from the Fig. 10 that as the welding current increases, the failure energy of the sample increases continuously, but the absorption of the tempered sample is greater than that has not been tempered. The maximum failure energy of the tempered and without tempered samples occurred when the welding current was 12 000 A, which was 56.94 kJ and 45.26 kJ, respectively.

Tako se dešava da je tačkasti spoj sočivastog šava bez otpuštanja manji nego otpušteni. Nakon otpuštanja nakon zavarivanja, može se dobiti veći tačkasti spoj. Prema radu A.S. Baskoro i dr. [22], prečnik sočivastog šava ima veliki uticaj na smicajnu silu zavarenog tačkastog spoja. Što je veća oblast spoja, to je veće opterećenje koje može da nosi spoj. Slika 8. pokazuje da srednja sila zatezanje - smicanje raste sa konstantnim povećanjem struje zavarivanja. U uslovima tretmana otpuštanjem maksimalna sila je 14.01kN kada je struja zavarivanja 12000 A, dok je maksimalna sila zatezanje – smicanje 12.84 kN u uslovima bez tretmana otpuštanja. Šta više srednja zatezno - smicajna sila kod uzoraka tretiranih otpuštanjem je veća nego bez otpuštanja uzorka pod istim uslovima. Slika 9 prikazuje da je rastojanje pomeranja (smicanja) otpuštenih uzoraka mnogo veće nego bez otpuštanja. Iz slike 10. može se videti da kada struja zavarivanja raste, energija loma uzorka kontinualno raste, ali i da je absobovana energija otpuštenog uzorka viša nego kod onih koji nisu otpušteni. Najveća energija loma otpuštenih i neotpuštenih uzoraka se postiže kada je struja zavarivanja 12000 A, odnosno iznosila je 56.94 kJ and 45.26 kJ, respektivno.

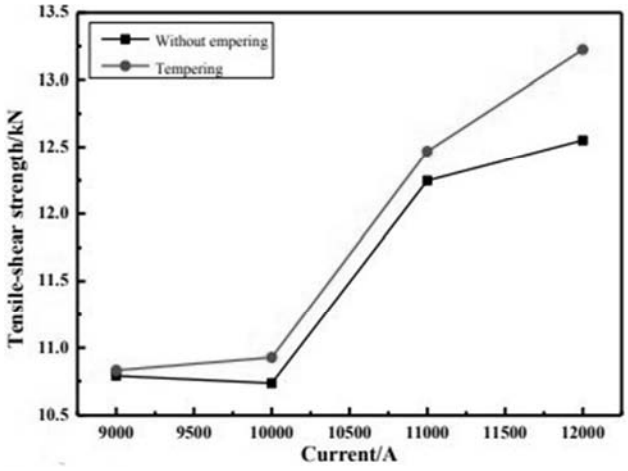

Figure 8. *Welding current tensile-shear force of joint before and after tempering*

Slika 8. *Zavisnost struja zavarivanja i zatezno–smicajna sila spoja pre i nakon otpuštanja*

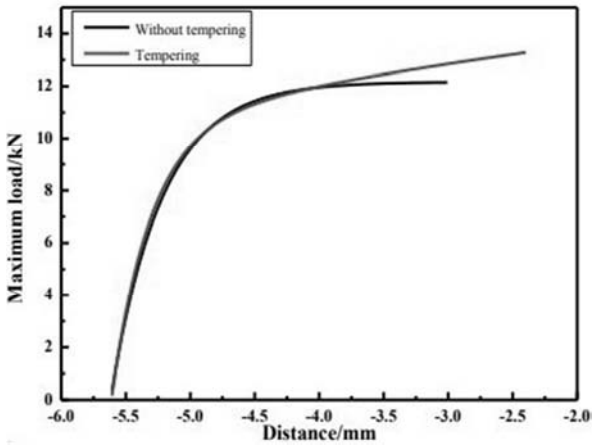

Figure 9. *Tensile-shear force-displacement curves of joint before and after tempering at the welding current: 12000A, welding time: 200ms, welding load: 3500N*

Slika 9. *Krive zavisnosti zatezno smicajne sile od pomeranja spoja (smicanja) pre i nakon otpuštanja pri struji zavarivanja od 12000A, vreme zavarivanja 200ms, sila zavarivanja 3500N*

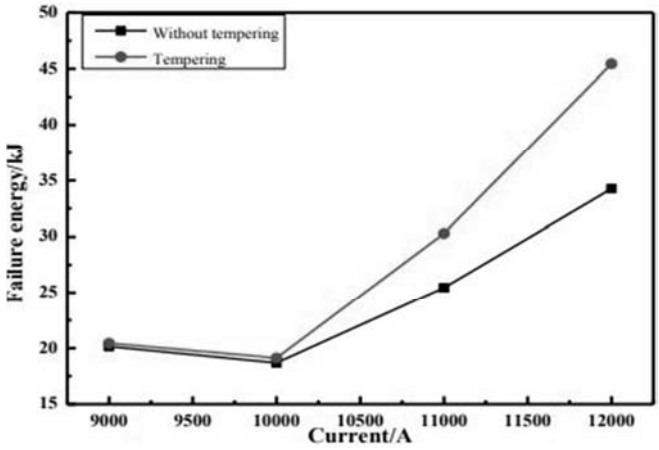

Figure 10. *Welding current- failure energy of joint before and after tempering*

Slika 10. *Zavisnost struje zavarivanja – energija loma pre i nakon otpuštanja*

The above results indicate the tempering treatment has a great influence on the mechanical properties of the spot welded sample. The change of tensile-shear strength is not only related to the joint size, but also related to the change of the microstructure in weld nugget area after tempering. Postweld tempering treatment can reduce the brittle quenching structure in the base metal, slow down the cooling rate of the spot joint and improve the mechanical properties [23].

3.3 Fatigue Properties

The spot welding parameters used in this fatigue test are 2 groups, of which the welding current is 12 000 A, the welding time is 200 ms, the pressure is 3 500 N, and the other was operated by post-weld tempering with the current is 6 000 A, and the time is 700 ms.

Gornji rezultati ukazuju da tretman otpuštanjem ima veliki uticaj na mehaničke osobine tačkasto zavarenih uzoraka. Promena zatezno smicajne čvrstoće nije jedino zavisna od veličine spoja, već zavisi i od promena mikrostrukture u oblasti sočivastog šava zavarenog spoja posle otpuštanja. Tretman otpuštanjem nakon zavarivanja može da smanji količinu krtih struktura zakaljivanja u osnovnom materijalu, usporavajući brzine hlađenja tačkastog spoja i time poboljša mehaničke osobine [23].

3.3. Osobine otpornosti na zamor

Dve grupe parametara zavarivanja su primenjene za ispitivanja otpornosti na zamor. Prva grupa ispitivana je na uzorcima zavarenim sa strujom zavarivanja od 12000 A,vremenom zavarivanja od 200 ms i pritiskom elektroda od 3500N, dok je druga grupa otpuštana nakon zavarivanja sa srtujom od 6000A u vremenu od 700ms.

Fig. 11 shows the fatigue curve of Spot welding joint before and after tempering. According to the equation (2-2), the joint fatigue strength of the tempered joint is 1.53 kN, and the fatigue strength without tempering is 1.18 kN. Postweld tempering treatment eliminates the residual stress of the joint and improving the fatigue strength of the joint.

Slika 11 pokazuje krive zamora tačkastih spojeva pre i nakon otpuštanja. Prema jednačini (2-2), zamorna čvrstoća otpuštenog spoja je 1.53 kN, a zamorna čvrstoća bez otpuštanja je 1.18 kN. Otpuštanje nakon zavarivanja eliminiše zaostale napone u spoju i poboljšava zamornu čvrstoću spoja.

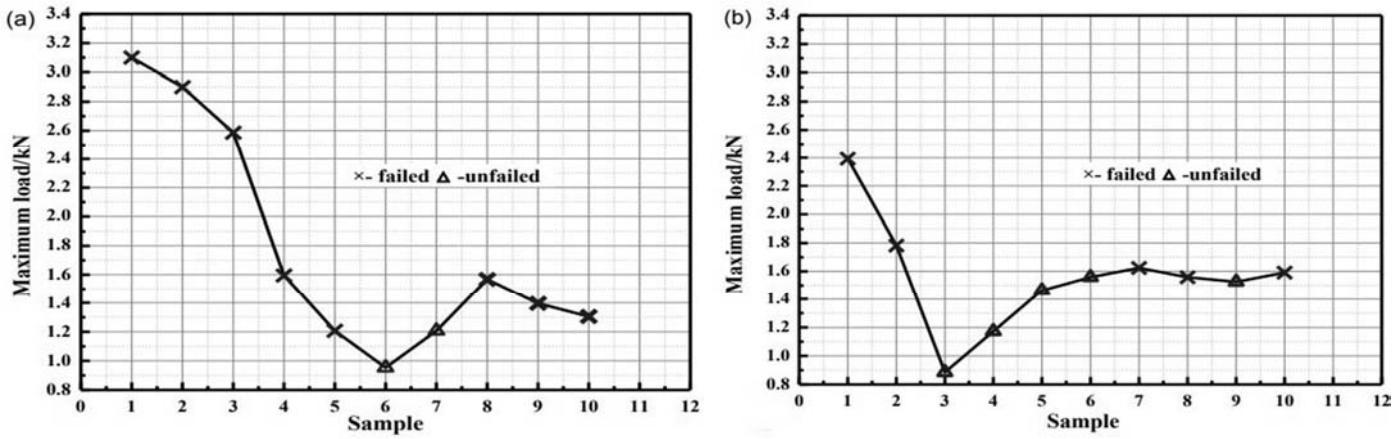

Figure 11. *Fatigue curve of DP600 spot welding joint, (a) Fatigue curve of DP600 spot welding joint with tempering, (b) Fatigue curve of DP600 spot welding joint without tempering*

Slika 11. *Kriva ispitivanja zamaranjem za tačkasti zavaren spoj za čelik DP600, a) Kriva zamaranja za tačkasti zavaren spoj za čelik DP600 sa otpuštanjem, b) Kriva zamaranja za tačkasti zavaren spoj za čelik DP600 bez otpuštanja*

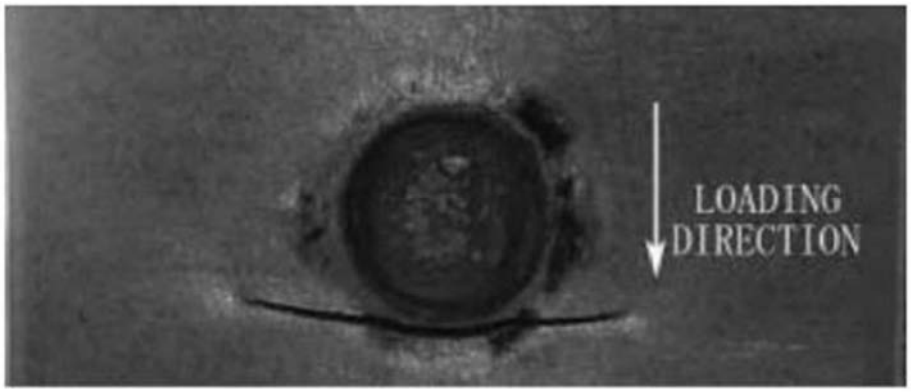

Figure 12. *Image of the sampled joint after fatigue testing*

Slika 12. *Slika uzorka spoja nakon ispitivanja zamorom*

Post-weld tempering treatment eliminates the residual stress of the joint and improving the fatigue strength of the joint. Whether the welded joint is tempered or not, it is found the cracks are generated near the weld heat affected zone, as shown in Fig. 12. The crack extends outward from the nugget boundary extending to the base material region and perpendicular to the loading direction. It indicates that the boundary between the base material and the weld nugget is the tip of the crack, and there is a large stress concentration near the heat affected zone.

Tretman otpuštanja nakon zavarivanja uklanja zaostale napone spoja i poboljšava zamornu čvrstoću spoja. Bez obzira da li je otpušten ili nije, konstatovano je da se prsline stvaraju blizu zone uticaja toplote, kao što je prikzano na slici 12. Prslina se prostire spolja od granice sočivastog šava, šireći se u oblast osnovnog materijala poprečno na pravac opterećenja. To ukazuje da je granica između osnovnog materijala i sočivastog šava u stvari vrh prsline, i da postoje velike koncentracije napona uz zonu uticaja toplote.

4. Conclusions

The effect of post-weld heat treatment on the performance of DP600 resistance spot welding joint is investigated. The following conclusions are made.

1. Post-weld tempering treatment brings the change of microstructure, tempered martensite occurred in the nugget, which reduces the microhardness of the weld nugget;

2. By post-weld tempering, we can obtain a larger spot joint and the mechanical properties, like tensile-shear strength and failure energy, is improved;

3. Post-weld tempering treatment eliminates the residual stress of the joint and improving the fatigue strength of the joint. All of the fatigue crack extends outward from the nugget boundary extending to the base material region and perpendicular to the loading direction.

Acknowledgements

The authors would like to acknowledge Dr. Hong Li for guiding the whole research. We also would like to acknowledge the financial support provided by Fundamental Research Funds for Beijing Municipal Universities (PXM2019_014204_500032)

4. Zaključci

Efekat termičke obrade nakon zavarivanja na osobine elektrootporno zavarenog spoja čelika DP600 je ispitivana i prikazana u radu. Sledeći zaključci mogu da se izvedu.

1. Tretman otpuštanjem nakon zavarivanja dovodi do promene mikrostrukture, otpušteni martenzit se javlja u sočivastom šavu, čime se smanjuje njegova mikrotvrdoća.

2. Primenom otpuštanja nakon zavarivanja dobija se veći tačkasti spoj i mehaničke osobine, kao zatezno-smicajna čvrstoća i energija loma se poboljšavaju.

3. Tretman otpuštanjem nakon zavarivanja eliminiše zaostale napone spoja i poboljšava zamornu čvrstoću spoja. Sve zamorne prsline šire se van granica sočivastog šava, šireći se u oblast osnovnog materijala i poprečno na pravac opterećenja.

Zahvalnica

Autori bi želeli da se zahvale Dr. Hong Li-u za vođenje celokupnog istraživanja. Takode se zahvaljujemo finansiskoj podršci obezbeđenu od strane Fundamental Research Funds for Beijing Municipal Universities (PXM2019_014204_500032)

References

[1] Evaluation Technologies on High strength steel sheet for Automobiles, Kobelco research institute, http://www.kobelcokaken.co.jp/en/example/c/index.html

[2] Nesa Raj S O Kumaran D and Sundar S S S P 2018 IOP Conference Series Materials Science and Engineering 402.

[3] Chabok A Van d A E and De Hosson J T M 2017 Materials & Design 124 171-182.

[4] Hsu T I Wu L T and Tsai M H 2018 The International Journal of Advanced Manufacturing Technology 53 152.

[5] Jianbin Chen Xinjian Yuan and Zhan Hu 2017 Journal of Manufacturing Processes, 30 396-405.

[6] Mousavi Anijdan S H Sabzi M and Ghobeiti-Hasab M 2018 Materials Science and Engineering: A 726 120-125.

[7] Eshraghi M Tschopp M A and Asle Zaeem M 2014 Materials & Design 56 387-397

[8] Wang B Hua L and Wang X 2016 International Journal of Advanced Manufacturing Technology 83(9-12) 1917-1926.

[9] Tao B H Li H and Meng X J 2011 National Welding Conference of China.

[10] Zhang H Qiu X and Xing F 2014 Materials & Design 55 366-372.

[11] W ilson H Farshid P and Veena S 2018 Metals 8(4) 199.

[12] Paveebunvipak K and Uthaisangsuk V 2018 Materials & Design 160 731-751.

[13] Liang X Yuan X and Wang H 2016 International Journal of Precision Engineering and Manufacturing 17(12) 1659-1664.

[14] Lara J H O and Ambriz R R 2017 Proceedings of the 17th International Conference on New Trends in Fatigue and Fracture.

[15] Wei S D Lv D X and Liu D 2014 Science and Technology of Welding and Joining 19 427-435.

[16] Zhao M S Chiew S P and Lee C K 2016 Journal of Constructional Steel Research 122 167-177.

[17] Pouranvari M and Marashi S P H 2010 Science and Technology of Welding and Joining 15(2) 149-155.

[18] Han X H Liu S L and Zhao Y Q 2013 China Railway Science 34(6) 84-88.

[19] Standards and Testing, http : // www . spottrack.eu / welcome/ standards - testing.jsp

[20] Zhang X G Yao F B and Ren Z H 2018 Materials 11 2310

[21] Wan X D Wang Y X and Zhang P 2014 ISIJ International 54 2375-2379

[22] Baskoro A S Trianda M R and Istiyanto J 2015 International Conference on Electrical Engineering & Computer Science. IEEE

[23] Wei S T and Lu S P 2017 Transactions of the China Welding Institution 08 118-138

Jacob Kleiman

Residual stress management: recent advances in engineering methods for non-destructive measurement and beneficial redistribution of residual stresses

Kontrolisanje zaostalih napona: razvoj najnovijih inženjerskih metoda za merenje bez razaranja i povoljnu preraspodelu zaostalih napona

CONTINUED FROM PREVIOUS ISSUE
Part 2

NASTAVAK IZ PREDHODNOG BROJA
2.deo

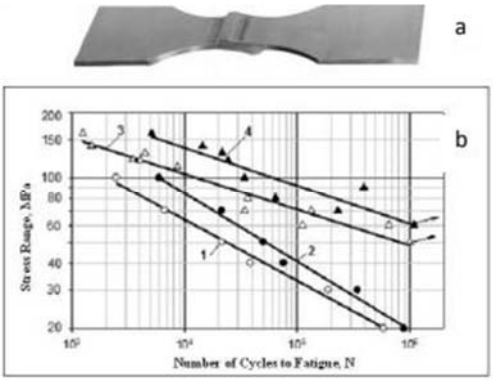

Figure 14. *Sample of overlap welded joint of 3 mm thick 6061-T6 aluminium alloy after application of UP* ***(a)*** *and fatigue curves of overlap welds of 3mm-thick 6061-T6 aluminium alloy* ***(b):*** *1 and 2–as-welded condition with 6 mm and 15 mm overlap respectively; 3 and 4–UIT/UP treated with 6 mm and 15 mm overlap respectively*

Slika 14. *Epruveta preklopnog zavarenog spoja debljine 3 mm od aluminijumske legure 6061-T6, nakon primene UP* ***(a)*** *zamorne krive preklopnog spoja od 3 mm;* ***(b)*** *1 i 2-preklopi od 6 i 15 mm u izvornom stanju; 3 i 4-UIT/UP obrađene epruvete sa preklopima od 6 i 15 mm, respektivno*

Specimens were subjected to axial loading at R=0 until complete specimen failure.The results of fatigue testing of the overlap welds prepared from 3mm-thick 6061-T6 aluminium alloy are illustrated in Fig. 14b.

As can be seen from Fig. 14b, the data for both overlap welds of 3mm-thick 6061-T6 aluminium alloy that were treated by UP are located considerably higher (lines 3 and 4 in Fig. 14b) then the data of “as-welded” samples (lines 1 and 2 in Fig. 14b). At 10,000 cycles of fatigue, an increase in the stress range was achieved by a factor of ~2 for overlap size of 6 mm and a factor of ~2.3 for the 15 mm overlap. At the same time, the number of cycles to fatigue increased ~ 6 times for the 6 mm overlap, and ~10 times for the 15 mm overlap.

In a different study, the influence of the ultrasonic peening treatment was evaluated for 5083 type aluminium alloy samples welded in two different configurations as shown in Fig. 15 and using different welding processes.

Epruvete su jednoosno opterećene pri odnosu napona R=0, do potpunog loma epruvete. Rezultati ispitivanja zamora zavarenih spojeva sa preklopom, napravljenih od 6061-T6 legure debljine 3 mm su prikazani na Slici 14b.

Kao što se može videti sa Slike 14b, podaci za oba preklopna spoja od legure 6061-T6, debljine 3 mm, koja je obrađena ultrazvučnim sačmarenjem (linije 3 i 4 na Slici 14b) se nalaze značajno iznad podataka dobijenih za epruvete u početnom stanju (linije 1 i 2 na slici 14b). Pri broju zamornih ciklusa od 10,000, faktor uvećanja napona koji je dostignut za preklapanje od 6 mm je iznosio ~2, dok je za preklapanje od 15 mm iznosio ~2.3. Istovremeno, broj zamornih ciklusa se povećao ~6 puta za preklop od 6 mm, i ~10 puta za preklop od 15 mm.

Druga studija se bavila uticajem ultravzučnog sačmarenja na aluminijumsku leguru 5083, pri čemu su korišćene epruvete sa dve različite konfiguracije, koje se mogu videti na Slici 15. U ovoj studiji su korišćeni različiti postupci zavarivanja.

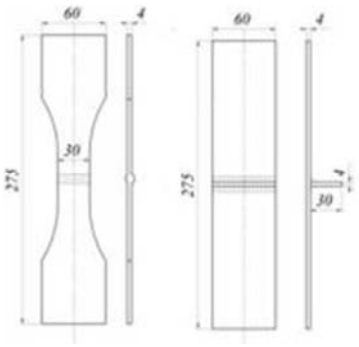

Figure 15. *Drawings of welded specimens in butt-weld and T-joint configurations*

Slika 15. *Crteži zavarenih epruveta sa sučeonom i ugaonom konfiguracijom*

The results of fatigue testing of these samples, using axial loading and R=0, in "as-welded" condition and after UP treatment are shown in Fig. 16. As can be seen from Fig. 16, the data for samples welded in both configurations that were treated by UP are located considerably higher then the data of "as-welded" samples.

Rezultati ispitivanja zamora za ove epruvete, pri jednoosnom opterećenju i R=0, u početnom stanju, kao i nakon obrade UP, su prikazani na Slici 16. Kao što se može videti sa slike, vrednosti za obrađene epruvete su daleko iznad vrednosti za epruvete u početnom stanju.

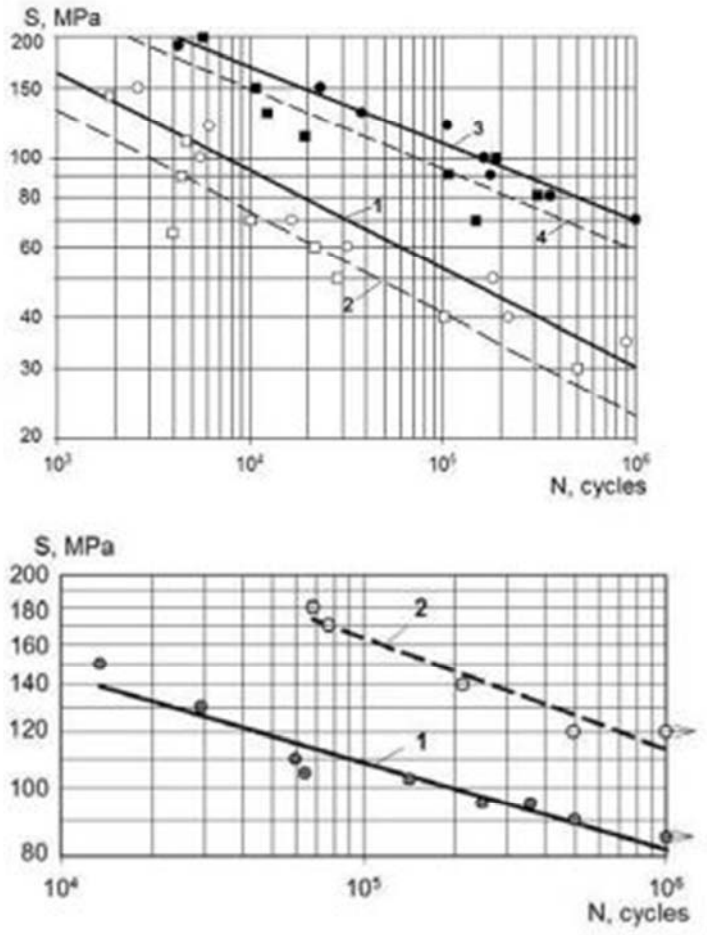

Figure 16. *Results of fatigue testing of samples made from 5083 alloy.* ***a)*** *butt- welded (as in Fig. 16a): 1, 2- in as-welded condition; 3, 4- after UP. 1, 3 – technology of welding A; 2, 4 – technology of welding B;* ***b)*** *T-joint weld (as in Fig. 16b): 1- in as-welded condition; 2 - after UP*

Slika 16. *Rezultati zamornih ispitivanja epruveta od legure 5083.* ***a)*** *sučeoni spoj (kao na slici 16a); 1,2 – početno stanje; 3,4 – nakon UP; 1,3 – tehnologija zavarivanja A; 2,4 – tehnologija zavarivanja B;* ***b)*** *T-spoj (kao na slici 16b): 1 – početno stanje; 2 – nakon UP*

At 10,000 cycles of fatigue, a ~54% increase in the stress range was achieved for the butt-welded samples and 30% for the T-joint samples. The fatigue life was also increase considerably, i.e. the number of cycles to fatigue increased ~ 12 times for both welded configurations.

4.4 Ultrasonic Underwater Peening (UUP) of Welded Structures

An ultrasonic peening system was designed and built for applications under water [29], [30]. The system (Fig. 17) looks similar to the basic UP systems shown in Fig. 10, but actually is very different in design.

Pri broju ciklusa od 10.000, postognuto je povećanje opsega napona od ~54% u slučaju sučeonih, i ~30% u slučaju T-spojeva. Zamorni vek je takođe značajno produžen, odnosno broj ciklusa je povećan ~12 puta za obe konfiguracije.

4.4 Podvodno ultrazvučno sačmarenje (Ultrasonic Underwater Peening – UUP) zavarenih konstrukcija

Sistem ultrazvučnog sačmarenja razvijen za primenu pod vodom [29, 30] je prikazan na slici 17 i izgleda slično kao i klasičan UP sistem prikazan na Slici 10, iako je zapravo veoma drugačije konstruisan.

Figure 17. *The ultrasonic system UltraPeen for underwater ultrasonic peening (UUP)*

Slika 17.*Sistem za ultrazvučno sačmarenje UltraPeen za podvodnu primenu*

Specially selected anti-corrosion materials were used in the design of the underwater UP instrument. The length of the cable connecting the peening gun to the generator can be adjusted to allow for treatments underwater at depths up to 30 meters or, if required, with certain modifications, even deeper. Acoustic pump principle is used in the originally developed system for water cooling of the transducer. The developed UP system allows for improvement treatments at four different power levels and is using replaceable working heads that come in various configurations with variable numbers of pins, depending on the application. Fig. 18 shows the process of underwater welding (Fig. 18a) followed by ultrasonic peening using the UUP system in manual treatment by an operator (Fig. 18b).The system was also operated in an automated mode, without the help from an operator.

Posebno odabrani antikorozivni materijali su korišćeni pri izradi instrumenata za podvodno ultrazvučno sačmarenje. Dužina kablova koji povezuju pištolj sa generatorom se može prilagoditi radu pod vodom na dubini do 30 metara, ili po potrebi i sa određenim modifikacijama, za još veće dubine. Princip akustične pumpe je primenjen na ovaj sistem kako bi se omogućilo vodeno hlađenje sonde. Ovako razvijen UP sistem omogućava poboljšanje u četiri različita nivoa snage i koristi zamenljive radne glave koje postoje u velikom broj različitih konfiguracija sa promenljivim brojem pinova, u zavisnosti od primene. Slika 18 prikazuje proces podvodnog zavarivanja (Slika 18a), praćen ultrazvučnim sačmarenjem primenom UUIP sistema, od strane operatera (Slika 18b). Ovaj sistem takođe može da radi u automatskom režimu, bez pomoći operatera.

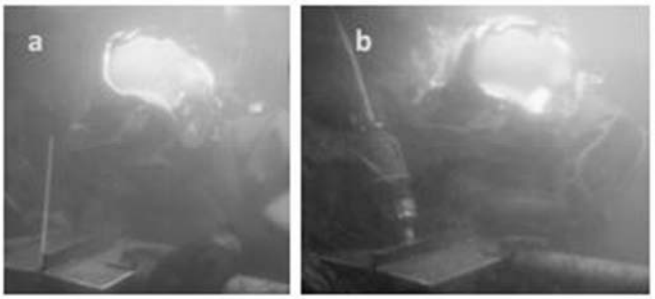

Figure 18. *The process of underwater ultrasonic peening using UltraPeen system. a) underwater welding process; b) Manual UP treatment of the welded sample by an operator;*

Slika 18. *Proces podvodnog ultrazvučnog sačmarenja primenom UltraPeen sistema. a) podvodno zavarivanje; b) ručna UP obrada zavarenog dela od strane operatera;*

To evaluate the efficiency of the new UltraPeen® technology and equipment for underwater ultrasonic peening (UUP) of welded elements, a study was conducted in which thirty four large-scale welded samples were produced (Fig. 19a) and fatigue tested after underwater UP treatment.

Kako bi se ocenila efikasnost nove UltraPeen® tehnologije i opreme za podvodno ultrazvučno sačmarenje, sprovedena je studija u okviru koje su napravljena 34 velika zavarena uzorka (Slika 19a**)**, koji su ispitani na zamor nakon podvodnog ultrazvučnog sačmarenja.

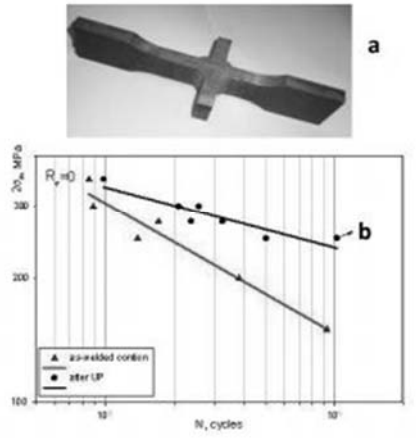

Figure 19. *Results of fatigue testing of samples welded and UP treated under water. a) Example of a non-load caring fillet sample prepared by underwater welding and following underwater UP treatment used in fatigue testing b) Results of fatigue testing of large metal samples in as-welded condition (triangles) and after the UUP treatment (solid circles).*

Slika 19. *Rezultati ispitivanja na zamor zavarenih uzoraka koji su obrađeni ultrazvučnim sačmarenjem pod vodom. a) primer nenosećeg ugaonog spoja pripremljenog podvodnim zavarivanjem nakon kojeg je sledila obrada pomoću UUP, za potrebe ispitivanja zamora b) rezultati ispitivanja na zamor velikih metalnih uzoraka u početnom stanu (trouglovi) i nakon UUP obrade (puni krugovi).*

Half of these samples were welded in open air and another half – underwater (Fig. 18a). Then, 50% of the samples from both batches were subjected to UUP (Fig. 18b) and all samples were fatigue tested. The results of the fatigue testing (Fig. 19b) had shown that the UUP provides significant fatigue improvement of welded elements, similar to what is observed for UP in air. The fatigue life of welded samples increased under the action of UUP 4-5 times depending on the level of applied stresses.

Polovina ovih uzoraka je zavarena na otvorenom, a druga polovina pod vodom (Slika 18a). Nakon toga, 50% uzoraka iz obe ture su podvrgnute obradi UUP metodom (Slika 18b), pri čemu su svi uzorci ispitani na zamor. Rezultati isptivanja zamora (Slika 19b) su pokazali da UUP obezbeđuje značajno poboljšanje zavarenih elemenata u pogledu otpornosi na zamor, slično kao što je uočeno kod ultrazvučnog sačmarenja na otvorenom. Zamorni vek zavarenih uzoraka je na ovaj način produžen 4-5 puta, u zavisnosti od nivoa delujućih napona.

Summary

In summary, it is safe to say that the concept of residual stress management is helping welders and the welding community to fully understand the effect of residual stresses by addressing major aspects of residual stresses in welds and welded structures. When the elements of the RSM are used together, the optimum performance of welded structures can be achieved.

The effect of residual stresses on material properties like fatigue, fracture, corrosion resistance and dimensional stability can be considerable and they, therefore, should be taken into account during design, fatigue assessment and manufacturing of parts and welded elements.

Substantial technological progress was made in the non-destructive measurement of applied and residual stresses by ultrasonic method. The UltraMARS-7 system incorporates new software and new functional capabilities, allowing evaluate the bulk, average through thickness stresses as well as the subsurface and surface stress changes. In addition it allows also evaluating the thickness of the materials and their Young modulus and Poisson ratio. The residual and applied stresses can be measured, calculated and their distribution displayed on the screen of the UltraMARS-7 instrument as continuous curves, with the option of transferring the data onto an USB device for further processing. The developed advanced ultrasonic method for non-destructive measurement of stresses and based on it portable instrument were used successfully in laboratory and field conditions for non-destructive measurement of applied and residual stresses in real parts and structural elements.

The ultrasonic peening technology was also matured with new models of the instrumentation for air and underwater treatments being developed and successfully demonstrated. The UP technology was successfully applied in construction industry, shipbuilding, railway and highway bridges, nuclear reactors, aerospace industry, oil and gas engineering and in other areas during manufacturing, in service inspection and repair of welded elements and structures.

Zaključci

Na kraju se može sa sigurnošću zaključiti da koncept kontrolisanja zaostalih napona pomaže zavarivačima da u potpunosti razumeju uticaj zaostalih napona u zavarenim spojevima i konstrukcijama. Kada se elementi RSM koriste istovremeno, može se ostvariti optimalno fukncionisanje zavarenih konstrukcija.

Uticaj zaostalih napona na osobine materijala, poput zamora, sklonosti ka lomu, otpornosti na koroziju i stabilnosti dimenzija može biti značajan i stoga se oni moraju uzeti u obzir tokom projektovanja, ocene zamornog veka i proizvodnje delova i zavarenih elemenata.

Značajan tehnološki napredak je načinjen u oblasti merenja metodama bez razaranja delujućih i zaostalih napona pomoću ultrazvuka. UltraMARS-7 sistem koristi novi softver i nove funkcije koje omogućavaju merenje prosečnog napona kroz celu debljinu, kao i na i pod površinom. Pored toga je takođe moguće oceniti debljinu materijala i njegov modul elastičnosti i Poasonov koeficijent. Delujući i zaostali naponi se mogu izmeriti, proračunati i prikazati na monitoru uređaja UltraMARS-7 u obliku neprekidnih kriva, sa opcijom prebacivanja podataka na USB uređaj za potrebe dalje obrade. Razvijene napredne ultrazvučne metode za merenje bez razaranja zasnovane na prenosivim uređajima su uspešno primenjene u laboratorijskim i terenskim uslovima za merenje delujućih i zaostalih napona u stvarnim delovima i konstrukcijama.

Tehnologija ultrazvučnog sačmarenja je takođe „sazrela“ sa primenom novih modela uređaja za obradu na vazduhu i pod vodom, koji su sa uspehom razvijeni i primenjeni u te svrhe. UP tehnologija je uspešno primenjena u građevinskoj industriji, brodogradnji, zatim u izradi železnice i mostova, nuklearnih reaktora, avioindustriji, naftnoj industriji i mnogim drugim oblastima, pri kontroli i reparaciji zavarenih elemenata i konstrukcija.

References / Literatura

[1] Trufyakov, V., Mikheev, P. and Kudryavtsev, Y., "Fatigue Strength of Welded Structures. Residual Stresses and Improvement Treatments", London. Harwood Academic Publishers GmbH. 1995.

[2] Kudryavtsev, Y., "Effect of Residual Stresses on the Endurance of Welded Joints", "International Institute of Welding", IIW Doc. XIII - 1568 - 94. 1994.

[3] Kleiman, J. and Kudryavtsev, Y., " Residual Stress Management in Welding: Residual Stress Measurement and Improvement Treatments", in Proceedings of ASME 2012 31st International Conference on Ocean, Offshore and Arctic Engineering, v 6: Materials Technology; Polar and Arctic Sciences and Technology; Petroleum Technology Symposium, Rio de Janeiro, Brazil, July 1–6, 2012, pp. 73-79

[4] Lu, J., Handbook of Measurement of Residual Stresses. Society for Experimental Mechanics. Edited by J. Lu. 1996. [5] Kleiman, J. and Kudryavtsev, Y., Ultrasonic Measurement of Residual Stresses in Welded Elements, 5 TH Annual CWA CanWeld Conference and IIW Congress, Westin Bayshore Hotel Vancouver, Canada, September 28 – October 1, 2014.

[6] Kudryavtsev, Y., Application of the ultrasonic method for residual stress measurement. Development of fracture toughness requirement for weld joints in steel structures for arctic service. VTT-MET. B-89. Espoo. Finland, (1985), pp.62- 76.

[7] Kudryavtsev, Y., Kleiman. J., and Gushcha, O., Residual Stress Measurement in Welded Elements by Ultrasonic Method, IX International Congress on Experimental Mechanics, Orlando, Florida, USA, June 5-8, (2000), pp. 954-957.

[8] Kudryavtsev, Y., Kleiman,. J. and Gushcha, O., Ultrasonic Measurement of Residual Stresses in Welded Railway Bridge, Structural Materials Technology: An NDT Conference. Atlantic Cit,. NJ. February 28-March 3, (2000), pp. 213-218.

[9] Kudryavtsev, Y., Kleiman, J., Gushcha, O., Smilenko, V., and Brodovy, V., Ultrasonic Technique and Device for Residual Stress Measurement, X International Congress and Exposition on Experimental and Applied Mechanics, Costa Mesa, California USA, June 7-10, (2004). pp. 1-7.

[10] Kudryavtsev, Y., Kleiman, J., Trufiakov, V. and Mikheev, P.. Expert System for Fatigue Assessment and Optimization of Welded Elements. Short Paper Proceedings of the Third World Congress of Structural and Multidisciplinary Optimization. Buffalo, New York, USA, May 17-21, 1999. Volume 2. p. 469-471.

[11] Kudryavtsev, Y. and Kleiman, J., Residual Stress Management: Measurement, Fatigue Analysis and Beneficial Redistribution, 2004 SEM X International congress and Exposition on Experimental and Applied Mechanics, June 7- 10, 2014, The Hilton Costa Mesa, Costa Mesa, CA, USA.

[12] Marquis, G. and Barsoum, Z., Fatigue Strength Improvement of Steel Structures by HFMI: Proposed Procedures and Quality Assurance Guidelines, International Institute of Welding IIW Document XIII-2453-13, 201.

[13] Kudryavtsev, Y., Korshun, V. and Kuzmenko, A., Improvement of Fatigue Life of Welded Joints by Ultrasonic Impact Treatment, Paton Welding Journal, 1989, No. 7. pp. 24- 28.

[14] Kudryavtsev, Y, Mikheev, P., and Korshun, V., Influence of Plastic Deformation and Residual Stresses Created by Ultrasonic Impact Treatment on Fatigue Strength of Welded Joints, Paton Welding Journal, 1995, No. 12. pp. 3-7

[15] Trufiakov, V., Mikheev, P., Kudryavtsev, Y. and Statnikov, E., Ultrasonic Impact Treatment of Welded Joints, International Institute of Welding, IIW Document XIII-1609- 95. 1995.

[16] Statnikov,E., Trufiakov, V., Mikheev, P. and Kudryavtsev, Y., Specifications for Weld Toe Improvement by Ultrasonic Impact Treatment. International Institute of Welding, IIW Document XIII-1617-96. 1996.

[17] Kudryavtsev, Y., and Kleiman, J., Increasing Fatigue Strength of Welded Elements and Structures by Ultrasonic Impact Treatment. International Institute of Welding. IIW Document XIII-2318-10. 2010.

[18] Kudryavtsev, Y., Kleiman, J., Lobanov, L., et al. Fatigue Life Improvement of Welded Elements by Ultrasonic Peening, International Institute of Welding. IIW Document XIII-2010- 04. 2004. 20 p.

[19] Kudryavtsev, Y., Kleiman, J., Lugovskoy, A., et al., Rehabilitation and Repair of Welded Elements and Structures by Ultrasonic Peening, International Institute of Welding, IIW Document XIII-2076-05. 2005. 13 p.

[20] Kudryavtsev, Y., Kleiman, J., Lugovskoy, A., and Prokopenko, G., Fatigue Life Improvement of Tubular Welded Joints by Ultrasonic Peening, International Institute of Welding. IIW Document XIII-2117-06, 2006. 24 p.

[21] Kudryavtsev, Y., Kleiman, J., Application of Ultrasonic Peening for Fatigue Life Improvement of Automotive Welded Wheels, International Institute of Welding, IIW Document XIII-2075-05, 2005, 9 p.

[22] Kudryavtsev, Y., Kleiman, J., Fatigue of Welded Elements: Residual Stresses and Improvement Treatments, Proceedings of the IIW International Conference on Welding & Materials, July 1-8, 2007, Dubrovnik, Croatia, P. 255-264.

[23] Haagensen, P., Progress Report on IIW WG2 Round Robin Fatigue Testing Program on 700 MPa and 350 MPa YS Steels, International Institute of Welding. IIW Document XIII-2081- 05, 2005.

[24] Marquis, G. and Björk, T., Variable Amplitude Fatigue Strength of Improved HSS Welds, International Institute of Welding, IIW Document XIII-2224-08, 2008.

[25] US Patent # 8,747,732 B2, Ultrasonic instrument for the deformation treatment of surfaces and weld joints, Jun. 10, 2014

[26] Kudryavtsev, Y., Kleiman, J., Kiryan,V., Klochkov, I., Fatigue Life Improvement of Welded Elements of Aluminum Alloys by Ultrasonic Impact Treatment, European Conference on Aluminum Alloys ECAA2011, Bremen, Germany October 5-7, 2011

[27] Klochkov, I, Berezin, I., Kudryavtsev, Y. and Kleiman, J., Fatigue Assessment of Fusion Welded Al Alloys: Scale Factor and Residual Stresses, European Conference on Aluminum Alloys ECAA2011, Bremen, Germany October 5-7, 2011.

[28] Klochkov, I., Kiryan, V., Berezin, I., Kudryavtsev, Y., Kleiman, J., Fatigue Improvement of AA2024 Aluminum Welded Joints by Ultrasonic Impact Treatment, MATERIALS SCIENCE ENGINEERING, Darmstadt, Germany, 25-27 September, 2012, https://www.spp1473.kit.edu/downloads/MSE2012_programm e.pdf

[29] Kleiman, J., Kudryavtsev, Y., and Lugovskoy, A., Underwater stress relieve and fatigue improvement by ultrasonic peening, Proceedings of the ASME 2012 31st International Conference on Ocean, Offshore and Arctic Engineering,OMAE2012, July 1-6, 2012, Rio de Janeiro, Brazil, Paper # 83469

[30] Kudryavtsev, Y., Kleiman, J., and Lugovskoy, A., Underwater Ultrasonic Peening of Welded Elements and Structures, Integrity, Reliability & Failure 2013, Funchal, Portugal, June 24-26, 2013.

Podsećamo Vas da je članarina za 2021.g ostala

nepromenjena i iznosi 3500,00 dinara.

Uplatom članarine stičete pravo na GRATIS godišnje izdanje

časopisa "ZAVARIVANJE I ZAVARENE KONSTRUKCIJE"

Tekući račun DUZS: 325-9500600002588-46

Informacije:

+ 381 (11) 2420-652

ČASOPIS ZAVARIVANJE I ZAVARENE KONSTRUKCIJE

Cenovnik oglasnog prostora u četiri uzastopna broja 2021

	A4	2/2	1/1	1/2	1/4	1/8
	dimenzije (mm)	2 x 210 x 297	210 x 297	180 x 120	90 x 120	90 x 60
DIN	crno/beli	-	39 000	23 000	16 000	10 000
	kolor	105 000	75 000	-	-	-

- U cene nije uračunat PDV 20%.
- Objavljivanje oglasa u samo jednom broju iznosi 30% od datih cena.
- Reklamni tekstovi: 25 % od cene površine crno/belih oglasa.
- Dostava materijala:
  - za crno-beli film ili CD (Adobe Photoshop / CorelDRAW);
  - za kolor film ili CD (Adobe Photoshop / CorelDRAW);
  - izrada filma sa CD: 10 % od cene angažovanog prostora.
- Na web prezetaciji DUZS-a, (www.duzs.org.rs), na strani Marketing, objavljuje se pregled firmi-oglašivača sa podacima o glavnim grupama proizvoda/usluga i adresom web prezetacije. Svi posetioci naše web prezentacije mogu da posete i web prezentacije oglašivača, preko aktivnih linkova koji se nalaze na ovoj stranici!

INDEKS OGLAŠIVAČA
ADVERTISERS INDEX

MESSER TEHNOGAS

WELD-ING

YASKAWA SLOVENIJA

HONEX

ELIMP

NEMINIK

WELDING & WELDED STRUCTURES, Quarterly review

Advertising prices for four successive numbers in 2021

	A4	2/2	1/1	1/2	1/4	1/8
	dimensions (mm)	2 x 210 x 297	210 x 297	180 x 120	90 x 120	90 x 60
EUR	black/white	-	840	432	336	240
	colour	2 640	1 680		-	-

- VAT 20% included.
- Advertising in one number only is 35% of the given prices.
- Commercial articles: 30 % of black/white advertising price.
- Print material:
  - for black/white CD (Adobe Photoshop / CorelDRAW)
  - for color CD (Adobe Photoshop / CorelDRAW).
- All the visitors of our web site may be linked to the advertisers' web site.

1. **ČLANARINA DUZS za 2021. godinu** …… **3.500 dinara**

   Članovima DUZS **GRATIS** godišnje izdanje časopisa "ZAVARIVANJE I ZAVARENE KONSTRUKCIJE"

2. **ČASOPIS "ZAVARIVANJE I ZAVARENE KONSTRUKCIJE" - 2021. godina u slobodnoj prodaji** (u cene je uračunat PDV 10%)**:**
   - cena pojedinačnog broja..... ……. 825 dinara
   - godišnja pretplata za 1 komplet brojeva godišnjeg izdanja…… 2.500 dinara
3. **ČASOPIS - stari brojevi** (u cene je uračunat PDV 10%)

   a) u slobodnoj prodaji:
   - cena pojedinačnog broja za 2019. godinu ..... ……..…… 500 dinara
   - cena pojedinačnog broja za prethodne godine…….....…... 250 dinara

   b) beneficirane cene za članove DUZS:
   - cena pojedinačnog broja za 2020. godinu (pouzećem ili preuzimanjem) .....……..... 400 dinara
   - cena pojedinačnog broja za prethodne godine (pouzećem ili preuzimanjem) ……..... Gratis
4. **Knjiga Organizacija i ekonomika zavarivačkih radova –** autor: prof. dr Zoran Radojević (uračunat PDV 10%) ……. 1.045 dinara
5. **Zbirke standarda OBEZBEĐENJE KVALITETA U ZAVARIVANJU, komplet 4 toma** 6.750 dinara